CHALMERS

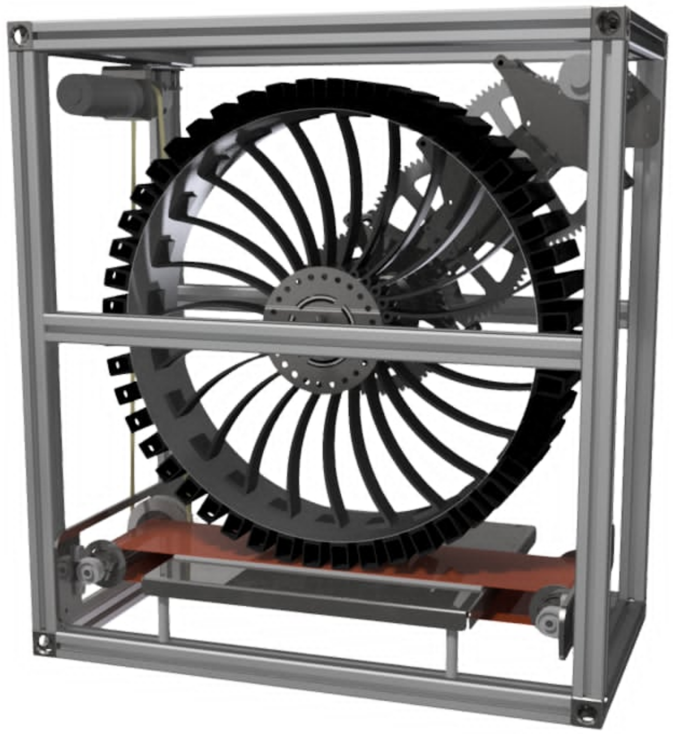

Design and manufacturing of a demonstrator of the tyre brush model

Bachelor's thesis in Mechanical Engineering and Automation & Mechatronics

Erik Ekdahl
Oscar Holm
Carl Nydewall
Fabian Steene

DEPARTMENT OF MECHANICS AND MARITIME SCIENCES

CHALMERS UNIVERSITY OF TECHNOLOGY
Gothenburg, Sweden 2026
www.chalmers.se

Bachelor's thesis 2026

Design and manufacturing of a demonstrator of the tyre brush model

Bachelor's thesis in Mechanical Engineering and Automation & Mechatronics

Erik Ekdahl
Oscar Holm
Carl Nydewall
Fabian Steene

Department of Mechanics and Maritime Sciences
Vehicle Engineering and Autonomous Systems
Vehicle Dynamics group
Chalmers University of Technology
Gothenburg, Sweden 2026

Design and manufacturing of a demonstrator of the tyre brush model
Bachelor's thesis in Mechanical Engineering and Automation & Mechatronics

Erik Ekdahl
Oscar Holm
Carl Nydewall
Fabian Steene

Supervisor: Bengt Jacobson, Department of Mechanics and Maritime Sciences
Examiner: Mats Jonasson, Department of Mechanics and Maritime Sciences

Bachelor's Thesis 2026
Department of Mechanics and Maritime Sciences
Vehicle Engineering and Autonomous Systems
Vehicle Dynamics group
Chalmers University of Technology
SE-412 96 Gothenburg
Telephone +46 31 772 1000

Cover: CAD model of the developed demonstrator

Typeset in LaTeX
Printing /Department of Mechanics and Maritime Sciences
Gothenburg, Sweden 2026

Design and manufacturing of a demonstrator of the tyre brush model
Bachelor’s thesis in Mechanical Engineering and Automation & Mechatronics
Erik Ekdahl
Oscar Holm
Carl Nydewall
Fabian Steene
Department of Mechanics and Maritime Sciences
Chalmers University of Technology

Abstract

The tyre brush model is widely used to describe tyre-road interaction, but physical demonstrations are uncommon. A real-world demonstrator was therefore developed to improve understanding of how tyre elements deform in the longitudinal direction under different operating conditions, including the formation of slip in the contact region.

A structured engineering design process was applied, including concept development and evaluation using systematic methods. The final system consists of a rotating wheel with flexible bristles and a moving belt representing the ground surface. The demonstrator is driven by electric motors and controlled using an Arduino-based system with motor drivers, allowing adjustment of operating conditions such as relative speed. This makes it possible to illustrate different slip scenarios in a clear and repeatable way.

The developed demonstrator partially visualises the intended real-world behaviour and represents a first step toward an educational tool for improving intuitive understanding of the tyre brush model. However, the demonstrator does not fully reproduce the expected brush model behaviour, as the bristles fail to continuously increase their deformation along the contact zone. Instead, they straighten toward the middle of the contact patch, which deviates from theoretical predictions. Despite this, certain key behaviours - such as increased bristle deformation at higher slip ratios and full loss of traction at low speed correlations - are observable. Future work is needed to address these shortcomings before the demonstrator can be used reliably as an educational tool.

Keywords: bristle, real-world demonstrator, slip, stick-slip, tyre brush model, tyre deformation

Acknowledgements

The authors would like to thank their supervisor and examiner for their valuable guidance, feedback, and support throughout the project. We also wish to thank Prototyplabbet at Chalmers for access to tools and manufacturing facilities that made the development of the demonstrator possible. Special thanks are extended to our fellow students Oscar Steen and Melker Folkesson who helped us with CNC manufacturing and to Magnus Gustaver for the Latex template that was used. Finally, we are grateful to our families and friends for their continuous encouragement and support during the course of this work.

Erik Ekdahl, Oscar Holm, Carl Nydewall, Fabian Steene, Gothenburg, May 2026

List of Acronyms

Below is the list of acronyms that have been used throughout this thesis listed in alphabetical order:

EPDM	Ethylene Propylene Diene Monomer
MM	Morphological Matrix
PETG	Polyethylene Terephthalate Glycol
RS	Requirement Specification
TPU	Thermoplastic Polyurethane

Nomenclature

Below is the nomenclature of parameters and variables that have been used throughout this thesis.

Parameters

R	Effective rolling radius of the wheel
μ	Coefficient of friction between tyre and road

Variables

S_x	Longitudinal slip ratio of the wheel
V_x	Forward velocity of vehicle
Ω	Angular velocity of the wheel
F_x	Longitudinal tyre force
F_z	Normal load on tyre

Contents

List of Figures

List of Tables

1
Introduction

Tyres play a central role in the performance and safety of road vehicles. Acceleration, braking, and steering are dependent on the forces generated in the contact between the tyre and the road surface. Although a tyre may appear to be a simple component, its behaviour is complex due to the interaction between rubber deformation, friction and slip. Understanding these phenomena is therefore fundamental to vehicle dynamics and tyre design. A common way to describe these interactions is the tyre brush model, which illustrates how forces arise in the tyre-road contact.

1.1 Aim

The aim of this project is to design and manufacture a real-world demonstrator of the tyre brush model. The demonstrator is intended to visualize how longitudinal tyre forces are generated through deformation and slip in the contact region between a tyre model and a simulated road surface.

The concepts of tyre deformation and slip can be difficult to understand intuitively when presented only through mathematical equations and diagrams. A real-world demonstrator can serve as an educational complement by translating the theoretical brush model into observable mechanical behaviour.

The intention is not to develop a fully accurate tyre test rig, but rather to create an educational demonstrator that illustrates the fundamental principles of the brush model in a clear and observable manner.

1.2 Project description

The real-world model developed in this project is intended to translate the theoretical brush model into an observable mechanical system. The interaction between the brush elements and the ground in the longitudinal direction is the primary focus of this demonstrator. This corresponds to a wheel in forward motion. By varying the relative motion between the wheel and the contact surface, the demonstrator can be used to illustrate both steady-state behaviour and conditions where slip occurs. A brush model describes force generation through an elastic material, the tyre in this case. Along with this, the model also demonstrates friction and slip [1, Ch. 2.2.3.1].

The main objective is therefore to make the bristles deform in a longitudinal manner, which shows the occurrence of slip. Possible secondary functions include representing lateral bristle deformation, such as the deformation that occurs when a wheel is steered, and simulating camber. These functions are considered extensions of the main concept.

1.3 Limitations

This work is subject to several limitations due to its pedagogical focus and the practical constraints associated with designing and manufacturing a real-world demonstrator. The demonstrator is intended to illustrate fundamental tyre-road contact rather than to provide precise measurements of tyre forces. The primary purpose is to create a visual and educational representation of the model.

The study focuses on force generation in the contact patch, and the primary objective is to investigate longitudinal forces. More complex tyre phenomena, such as lateral force generation, camber effects, combined slip and moment generation, are not included in the final scope of the project. Including these effects requires a more advanced mechanical design, additional control possibilities and more precise calibration.

The limitations are introduced to keep the project manageable and to ensure that the demonstrator remains focused on its primary educational purpose. Real tyres involve complex material properties, tread patterns, temperature-dependent effects, and other complex phenomena, which are not reproduced in the demonstrator. The demonstrator is a simplified version of the brush model to demonstrate the fundamental idea.

1.4 Research questions

The primary objective of the project is to design and construct a real-world demonstrator that illustrates the deformation behaviour of the tyre tread within the contact patch, as described by the brush model. Furthermore, the demonstrator should be constructed in a way that makes it suitable for educational environments.

To achieve this objective, the following research questions are addressed:

- How can the assumptions and mechanisms of the brush model be translated into a mechanical design suitable for a real-world demonstrator?
- What limitations does the real-world demonstrator have when compared to the theoretical brush model?

2
Theory

The brush model, originally developed as a theoretical concept in tyre dynamics and later discussed by H.Pacejka [2, Ch. 3.2] and B.Jacobson et al [1, Ch. 2.2.3.1], represents the tyre-road contact patch as a continuous row of elastic bristles that deform when in contact with the road surface. Each bristle represents a part of the tyre's rubber surface and develops a shear force as it is deformed.

In the brush model, the wheel's effective rolling radius R is assumed constant. The bristles deform and generate shear forces, but the wheel's overall circumference does not change. **Slip** occurs when the rotational speed of the wheel in the contact point does not match the forward speed of the vehicle. The longitudinal slip ratio is defined as

$$S_x = \frac{\Omega R - V_x}{|\Omega R|} \tag{2.1}$$

where V_x is the forward speed of the vehicle and Ω is the angular velocity of the wheel. At small slip ratios, all bristles remain stuck to the road surface in the **adhesion region**, and the longitudinal force grows approximately linearly with slip. As slip increases, bristles at the rear part of the contact patch reach the friction limit and begin to slide, while bristles at the front remain stuck. The sliding region gradually expands along the patch until eventually the entire contact patch is sliding. A typical slip curve is illustrated in figure **??** and a simplified side-view representation of the brush model is shown in figure 2.2.

The total longitudinal tyre force is limited by the available friction and cannot exceed μF_z where μ is the coefficient of friction and F_z is the normal load acting on the tyre. When the entire contact path is sliding, the longitudinal tyre force has reached its limit.

This model explains how longitudinal tyre forces are generated and provides the basis for the demonstrator, where the focus is on showing bristle deformation and slip in the longitudinal direction.

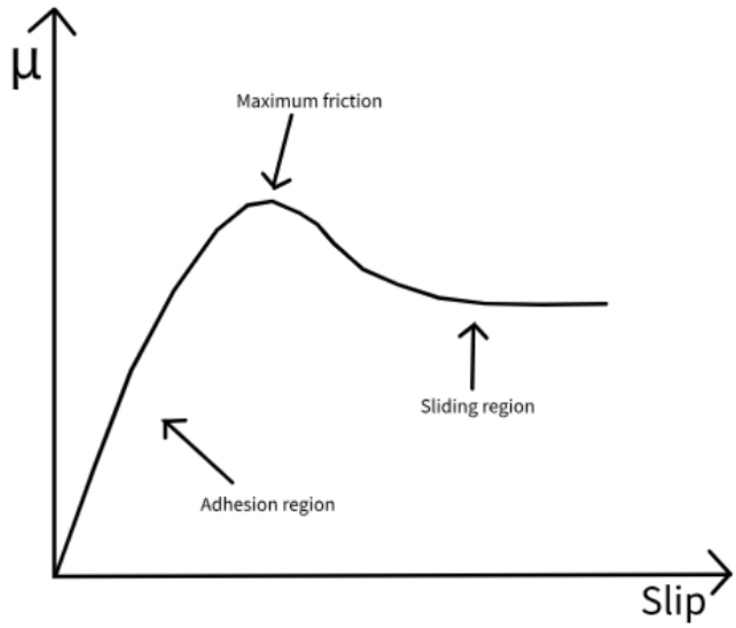

Figure 2.1: Slip curve

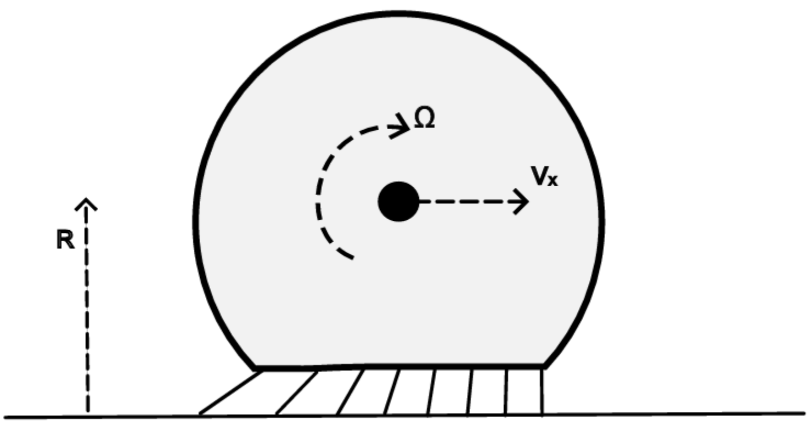

Figure 2.2: Simplified brush model seen from the side. Drawn for braked wheel without a sliding zone.

3
Methods

The methodology followed throughout the project mainly focuses on methods for concept development and evaluation, including structured idea generation and the use of evaluation matrices. These methods provide a systematic basis for exploring and comparing different concepts.

3.1 Concept development

The concept development phase consists of structured methods used to support the systematic exploration of possible solutions.

3.1.1 Tree of functions

A tree of functions is used to divide the overall project objective into smaller sub-functions. This helps clarify the essential system operations and creates a structured basis for further concept generation.

3.1.2 Requirement specification matrix

A requirement specification (RS) matrix is used to define and evaluate the criteria relevant to a product or system design. Requirements that are essential for the product to function and achieve its primary objectives are classified as required (R), while non-essential but desirable criteria are classified as desired (D) [3].

The desired criteria can further be ranked according to their importance. For example on a scale from 1 to 5, where higher values indicate greater priority. This allows different design criteria to be weighted and compared systematically. Defining requirements also makes it possible to assess whether they have been fulfilled and to establish measurable design targets.

3.1.3 Idea generation

Idea generation is used to create a broad range of potential sub-solutions for each of the sub-functions found in the tree of functions. The main benefit of idea generation is that it broadens the solution space and helps prevent premature fixation on a single solution early in the design process. Inspiration can also be gathered by studying similar products, technical solutions and relevant application environments, which may provide useful ideas.

The process begins with brainstorming, where multiple ideas are generated and explored without immediate evaluation. This encourages creativity and helps identify a wide range of possible design solutions.

The generated ideas are then discussed and compared in order to identify similarities, combine promising ideas and assess their strengths and weaknesses. Linking the ideas to specific sub-functions in the tree of functions helps maintain a systematic design process and ensures that all essential system functions are addressed.

3.2 Concept evaluation methods

The section describes the evaluation methods used in the project. The purpose of using these evaluation tools is to structure the work, while making documentation of the process easy and clear. Furthermore, they encourage the exploration of multiple concepts. Two evaluation methods were used: the morphological matrix and the elimination matrix.

3.2.1 Morphological matrix

A *morphological matrix* (MM) is used to generate and structure combinations of the sub-solutions generated during idea generation; these combinations are called concepts. Each sub-solution, linked to its respective sub-function allows for a large number of concepts to be explored systematically [4]. The method also allows incompatible combinations to be excluded, ensuring that only technically feasible solutions are considered.

3.2.2 Elimination matrix

An elimination matrix is used to evaluate concepts against a set of mandatory requirements. Each concept is compared to the RS, and the ones that do not meet all required criteria are removed [5]. In the matrix, a plus sign (+) indicates that the concept fulfils the criterion, a minus sign (-) indicates that it does not, and a question mark (?) indicates that fulfilment could not be determined at the concept stage. A concept is eliminated if it receives at least one minus sign. This method ensures that only concepts that fulfil the essential project requirements are carried forward in the development process.

4

Implementation

This chapter follows the structure defined in the Methods chapter and presents how the selected methods were applied in practice.

4.1 Implementation of concept development

The section covers the implementation and results of the creative part of concept development.

4.1.1 Tree of functions

The function tree is shown in figure 4.1. The dashed lines indicate functions that were not necessary for the final demonstrator.

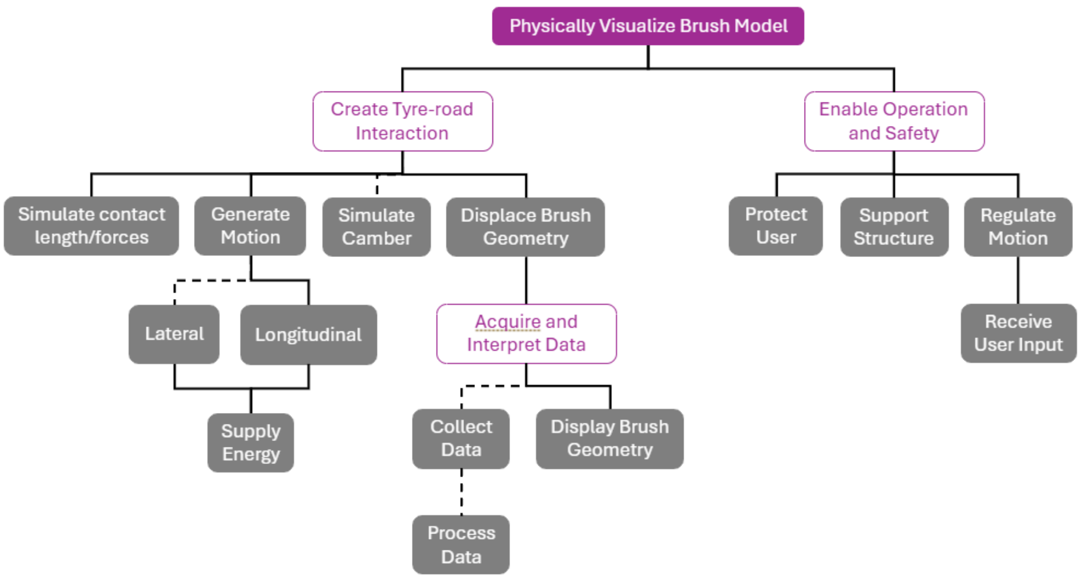

Figure 4.1: Tree of functions

4.1.2 Requirement specification matrix

The developed RS matrix is shown in table 4.1. Explanations of how the different requirements were derived, as well as how they are verified and tested, are provided in Appendix B. Requirements classified as R (required) were not assigned weights, since they represent binary pass/fail criteria that must be met regardless of priority. Weights were only assigned to desired (D) criteria to allow relative comparison between non-mandatory goals.

Table 4.1: Requirement specification matrix

No.	Criteria	Goal	R/D	W	Verification	Ref.
Functions						
	Physically Visualise Brush Model		R		Test	Brush Model
	Simulate Longitudinal Motion		R		Test	Brush Model
	Simulate Lateral Motion		D	2	Test	Brush Model
	Simulate Camber		D	3	Test	Brush Model
	Collect & Compare w. Theory	Val. var. 10%	D	4	Calculations	Supervisor
1. Performance						
1.1	Consistent slip relation	Var. 5%	D	5	Data collection	Supervisor
1.2	Clearly Visible Deformation	From 3 m	R		Test	Supervisor
1.3	Clearly Visible Deformation	From 5 m	D	2	Survey	Supervisor
1.4	Clearly Visible Slip Zone	From 3 m	D	3	Survey	Supervisor
1.5	Clearly Visible Slip Zone	From 5 m	D	2	Survey	Supervisor
2. Environment						
2.1	Env. Temperature	15–30 °C	R		Test	Prod. Plan.
3. Size						
3.1	Maximum L+W+H	2 m	R		CAD	Supervisor
3.2	Maximum L+W+H	1.5 m	D	2	CAD	Supervisor
4. Mass						
4.1	Max weight	25 kg	R		CAD	Supervisor
4.2	Max weight	15 kg	D	3	CAD	Supervisor
5. Ergonomics						
5.1	Maximum sound level	50 dB	D	3	Test	Supervisor
6. Safety						
6.1	Maximum sound level	80 dB	R		Test	Arbetsmiljöv.
6.2	Min. Projectile Debris		R		Supervisor Ass.	Prod. Plan.
6.3	Min. Risk of Fire		R		Supervisor Ass.	Prod. Plan.
6.4	Min. Risk of Elec. Shocks		R		Supervisor Ass.	Prod. Plan.
6.5	No Sharp Edges		R		Test	Prod. Plan.
6.6	Min. Risk of Burns		R		Supervisor Ass.	Prod. Plan.
6.7	Min. Pinch Hazard		R		Supervisor Ass.	Prod. Plan.
7. Material						
7.1	Brush with Elastic Properties		R		Test	Prod. Plan.
8. Production Cost						
8.1	Maximum cost	10 000 kr	D	5	Cost summery	Chalmers (M2)
9. Maintenance						
9.1	Replaceable Brush	≤30 min	R		Test	Prod. Plan.
9.2	Easily Replaceable Brush	≤10 min	D	4	Test	Prod. Plan.
10. Reuse and Recycle						
10.1	Easily Repairable		D	4	Supervisor Ass.	Prod. Plan.
10.2	Recyclable Bristles		D	3	Material Analysis	Prod. Plan.

4.1.3 Concept generation outcomes

The concept generation process resulted in a wide range of potential sub-solutions for the system's sub-functions. Due to the specific nature of the project, it was difficult to find directly comparable existing products. Instead, inspiration was taken from related mechanical systems and partial solutions.

For inspiration on designing a demonstrator, examples of existing teaching aids demonstrating mechanical deformation were examined. In particular, demonstrations of buckling end conditions were studied, as they provide a clear and intuitive way of visualising deformation. This was similar to the objective of the demonstrator in this project, which was to clearly illustrate brush deformation. Some solutions relied on simple deformable materials, allowing for intuitive and interactive demonstrations, while others used more rigid mechanical structures that offered greater repeatability and precision. These observations helped guide the early concept development.

Broader research into inducing displacement and motion identified the concept of metamaterials, which are materials that use variation in their internal structure to make deformation more predictable [6]. Examples include Adidas's topological 4D shoe-soles [7], and a Princeton article presents a metamaterial capable of producing movement without motors by combining the material structure with electromagnets [8]. In the brush model, similar principles could potentially be applied to create displacement in the bristles.

To generate additional ideas, the AI ChatGPT [9] was provided with the project specifications and instructions to generate solutions for the functions described in the functional structure. Solutions already thought of in earlier steps were flagged, and the AI was instructed:

> *"Give me new solutions that have not already been found by us, see attached picture"*

This ensured that no duplicates were included, and gave the AI a better understanding of the task. Many AI-generated solutions were non-viable and non-compatible with the RS, but some had potential and were added to the final table of sub-solutions.

Finally, all concepts from individual brainstorming, group brainstorming, research on existing solutions, and AI were compiled into a single table (see Fig. A.1).

4.2 Implementation of concept evaluation

The section covers the implementation and results regarding processing and filtering of the sub-solutions. It should be noted that the purpose of the different matrices was not to automatically produce an optimal solution, but rather to provide structure and support decision-making.

4.2.1 Morphological matrix results

The MM was created using sub-functions from the tree of functions along with their corresponding sub-solution alternatives, which were assigned during the idea generation phase. To simplify the process, a MM tool [10] was used.

The first step in the process was setting limitations in order to eliminate invalid solutions. The website used to create the morphological matrices includes a function that allows the user to prohibit combinations of sub-solutions. using this tool ensured that only technically feasible solution sets were made.

Initially, all sub-functions and their respective sub-solutions were included in the matrix. This resulted in a comprehensive solution space, which was visually complex and was therefore changed. To reduce volume, the functions “Data collection,” “Process data,” and “Protect user” were excluded, mostly because the limitations of the project were not yet final. The excluded functions were not included during the concept evaluation phase, but were intended to be considered later in the process.

The next step was to generate a second draft of the matrix. In this phase, solutions were generated using a Pragmatic strategy setup (see Fig. A.2). Sub-functions were ranked based on importance. Thereafter, sub-solutions were removed based on the rankings of the sub-functions, meaning more sub-solutions got removed from the less important categories. It is an effective way of quickly reducing the number of concepts, however, this approach resulted in a discrepancy between the number of sub-solutions in each sub-function category. The vast majority of sub-functions had only one corresponding sub-solution, whilst the three most important ones had between two and five each as shown in figure A.3.

Because of this, a manual correction was made to the matrix, which resulted in a more controlled elimination of sub-solutions and an iterated MM shown in figure A.4. This enabled a wider distribution of sub-solutions within sub-function categories that could benefit from multiple alternatives to generate technically distinct concepts. The final MM included more evenly distributed sub-solution alternatives, reducing the dominance of individual sub-functions and sub-solutions.

To further improve clarity, a reduced MM was created, as illustrated in figure 4.2. This matrix was based on the final version but with certain sub-function categories removed.

Morphological Matrix

Sub-Functions	Sub-Solutions		
Displaceable brush geometry	Flexible bristles	Magnets	Meta material
Display brush deformation	Synched stroboscopic lighting	Visible as is	
Display slip zone	Visible as is	LED indicator	
Simulate road contact	Flexible tyre material	Magnets	
Generate lateral motion in brush	Electromagnets	Belt driven contact surface	

Figure 4.2: Final morphological matrix

Sub-solutions that were lone in their sub-function categories were verified against RS, making it possible to remove the sub-function category. Additionally, the two sub-solutions in the support structure category were verified against the RS and subsequently removed from the list. Before the removal of the support structure category there were $2^5 \cdot 3 = 96$ possible combinations where the exponent represents the number of sub-function categories with two alternatives each, and the factor of three corresponds to the sub-function with three alternatives. The removal of the support structure category reduced the number of concepts to $96/2 = 48$, resulting in a more manageable set. This was done because it was considered more appropriate to determine the frame material at a later stage, when more details of the final concept were known.

Compared to the initial version, the final set of concepts provided a clearer and more balanced matrix, making it more suitable for continued development. This version was therefore used when further developing the demonstrator concept.

4.2.2 Elimination process

The next step in the concept evaluation phase was carried out using the elimination matrix, shown in table 4.2, to systematically reduce the number of remaining concept alternatives. Only the most important requirements from the RS matrix were included.

Table 4.2: Elimination matrix

Sol.	Decision	Physically Visualise Brush Model	Simulate Longitudinal Motion	Clearly Visible Deformation 3m	Env. Temp. 15–30°C	Max L+W+H 2m	Max weight 25kg	Max sound 80dB	No Sharp Edges	Brush Elastic Properties	Replaceable Brush ≤30min
1	Keep	+	+	?	+	+	+	+	+	+	+
2	Elim.	+	+	?	+	+	+	+	+	+	+
3	Keep	+	+	?	+	+	+	+	+	+	+
4	Elim.	+	+	?	+	+	+	+	+	+	+
5	Keep	+	+	?	+	+	+	+	+	+	+
6	Elim.	+	+	?	+	+	+	+	+	+	+
7	Keep	+	+	?	+	+	+	+	+	+	+
8	Elim.	+	+	?	+	+	+	+	+	+	+
9	Keep	+	+	+	+	+	+	+	+	+	+
10	Elim.	+	+	+	+	+	+	+	+	+	+
11	Keep	+	+	+	+	+	+	+	+	+	+
12	Elim.	+	+	+	+	+	+	+	+	+	+
13	Keep	+	+	+	+	+	+	+	+	+	+
14	Elim.	+	+	+	+	+	+	+	+	+	+
15	Keep	+	+	+	+	+	+	+	+	+	+
16	Elim.	+	+	+	+	+	+	+	+	+	+
17	Elim.	–									
18	Elim.	–									
19	Elim.	–									
20	Elim.	–									
21	Elim.	–									
22	Elim.	–									
23	Elim.	–									
24	Elim.	–									
25	Elim.	–									
26	Elim.	–									
27	Elim.	–									
28	Elim.	–									
29	Elim.	–									
30	Elim.	–									
31	Elim.	–									
32	Elim.	–									
33	Keep	+	+	?	+	+	+	+	+	+	+
34	Elim.	+	+	?	+	+	+	+	+	+	+
35	Keep	+	+	?	+	+	+	+	+	+	+
36	Elim.	+	+	?	+	+	+	+	+	+	+
37	Keep	+	+	?	+	+	+	+	+	+	+
38	Elim.	+	+	?	+	+	+	+	+	+	+
39	Keep	+	+	?	+	+	+	+	+	+	+
40	Elim.	+	+	?	+	+	+	+	+	+	+
41	Keep	+	+	+	+	+	+	+	+	+	+
42	Elim.	+	+	+	+	+	+	+	+	+	+
43	Keep	+	+	+	+	+	+	+	+	+	+
44	Elim.	+	+	+	+	+	+	+	+	+	+
45	Keep	+	+	+	+	+	+	+	+	+	+
46	Elim.	+	+	+	+	+	+	+	+	+	+
47	Keep	+	+	+	+	+	+	+	+	+	+
48	Elim.	+	+	+	+	+	+	+	+	+	+

The creation of the final morphological matrix resulted in the exclusion of many sub-solutions. It was a necessary step to reduce the number of concepts to a manageable size. However, these exclusions were often based on the same criteria later applied in the elimination matrix. In addition, the large number of sub-solution categories meant that only one or two sub-solutions remained within almost every category. Together, these factors led to a list of concepts that were very similar to one another and either passed or failed the elimination matrix based on the same criteria.

At an early stage, the sub-solution involving magnets for simulating road contact was eliminated. It was concluded that it would not mirror the theory well enough. While the method had many benefits, the discrepancies in force direction and behaviour made it unsuitable for this project.

After the elimination process, only five sub-function categories contained more than one viable sub-solution. Furthermore, these categories had limited interaction with one another. It was therefore decided that the remaining sub-solutions were to be evaluated through discussion. The remaining functions and their corresponding sub-solutions were:

- **Displaceable brush geometry** - Flexible bristles, Magnets, Meta material
- **Display brush deformation** - Synced stroboscopic lighting, Visible as is
- **Display slip zone** - Visible as is, LED indicator
- **Generate lateral motion in brush** - Electromagnets, Belt driven contact surface
- **Support structure** - Metal frame, Wooden frame

4.2.3 Evaluation of final sub-solutions

The use of magnets to deform the bristles was considered more suitable in a fully magnetic system, with no mechanical contact. Only choosing magnets for the deformation, and not for all the sub-functions where it was an option, removed the main advantages of using this approach while adding unnecessary complexity.
This limitation should ideally have been identified in the morphological matrix but was overlooked due to the large number of possible combinations. Similarly, the idea of using electromagnets to induce lateral motion was discarded for largely the same reasons. In addition, since the method for generating longitudinal motion in the brush had already been selected, it was considered more appropriate to use the same method for both longitudinal and lateral motion. As a result, all concepts involving magnetic and electromagnetic solutions were discarded. These concepts are the ones that have been eliminated in the elimination matrix even though they fulfilled all requirements.

Rather than selecting a single sub-solution for the visualisation of the brush deformation, the sub-solution alternatives were assigned a priority ranking. The preferred option was to make the phenomenon visible "as is" without additional aids. If this proved to be unfeasible, stroboscopic lighting could be implemented as a secondary solution to enhance visibility. A similar prioritisation was applied to the visualisation of the slip zone, where direct visibility was preferred, with an LED strip as a backup option to indicate where slip occurs along the contact length of the wheel.

For the brush geometry, the two remaining alternatives were both retained for further development. Since the component was to be easily interchangeable, both options could be explored in parallel. The metamaterial structure offered advantages in terms of improved visibility of the internal structure and the possibility of tailoring the flexibility of different regions of the structure. Although a metamaterial allows for more customizability, a solid flexible material, provides a simpler and potentially more robust solution, with a lower risk of fatigue-related issues.

As the support structure, a metal solution was chosen. Compared to a wooden frame, the metal frame offered greater structural rigidity and reduced concerns related to wear and fire safety.

4.3 Selected concept

Based on the concept evaluation, a final set of sub-solutions was selected for further development. The selection was made by combining feasibility, simplicity, and how well each solution aligned with the project objectives.

For the brush system, a flexible solution was selected, where either a compliant material or a metamaterial-inspired structure could be used. Both alternatives were retained since they offered different advantages. The visualisation of bristle deformation and slip was primarily based on direct observation, as this provides the most intuitive understanding of the phenomena.

The mechanical system should generate longitudinal bristle deformation using a belt-driven contact surface, providing stable and controllable motion under load. The potential addition of lateral motion in the bristles should be generated using the same method. The road interaction was modelled using a flexible material for the tyre.

System control should be implemented using a power controller to regulate motor speed. Furthermore, camber variation should be achieved through a manual adjustment mechanism, enabling controlled changes in wheel angle without introducing unnecessary complexity. Other user input is handled through simple buttons, and the system's power is supplied from a standard wall outlet to ensure continuous operation. Finally, a metal frame was selected as the support structure to provide sufficient stability.

5

Design and Prototype development

The chapter presents an initial overview of the demonstrator. Then, it goes further into the thought process behind each of the main components. Finally, the demonstrator is assessed in regards to the requirement specification matrix.

5.1 Final design

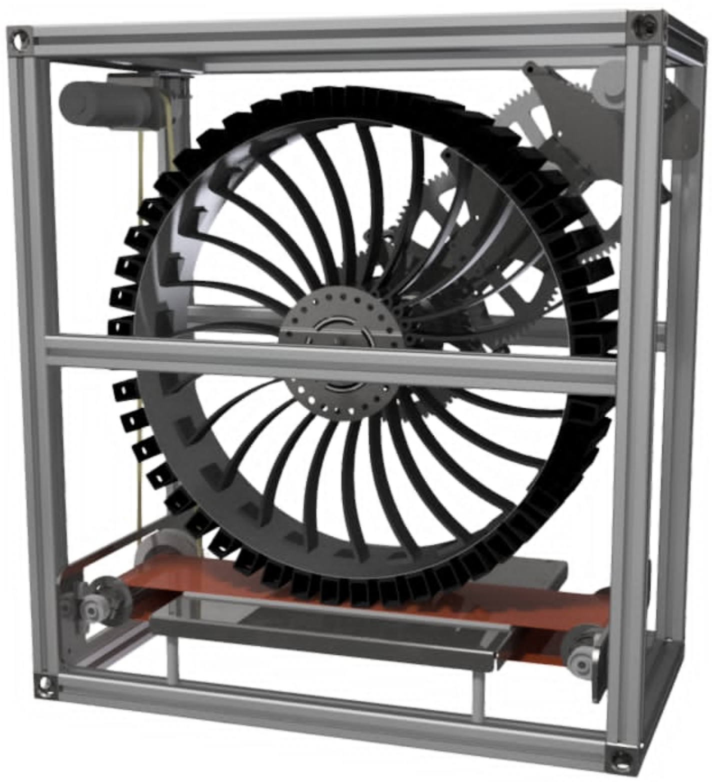

Figure 5.1: CAD model of the demonstrator

5.1.1 System overview

The demonstrator, seen in figure 5.1, consists of two main mechanical subsystems: a rotating wheel and a moving belt representing the road surface. The relative motion between these two components is used to simulate slip conditions and study bristle deformation at the contact surface. The frame was constructed using modular aluminium profiles with railings. The structure supports the wheel assembly, belt system, motors, and electrical components.

Figure 5.2: CAD model of the frame

The wheel design consists of a spoke-based structure using 24 elements 3D-printed with *Thermoplastic Polyurethane* (TPU) 95A. The spokes act as compliant elements, allowing the wheel to flatten locally under load and create a contact length of approximately 200 mm between the bristles and the belt surface. This contact length is sufficient to place approximately six bristles in contact with the belt, which is necessary for the stick-slip transition to be observable across the contact patch. At the centre of the wheel, a metal hub is used as the main power-transferring component and at the outer perimeter, the spokes are connected using a thin aluminium sheet. The bristles mounted to the aluminium sheet were designed as the primary visualisation element of the demonstrator and therefore became one of the most important components of the system. In total, there are 48 3D-printed bristles, made from TPU 95A. Their internal structure reduces stiffness, increasing visible deformation.

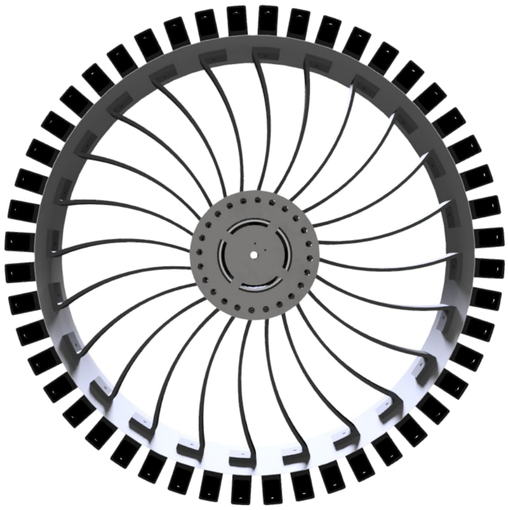

Figure 5.3: CAD model of the wheel

The belt system was designed to simulate the road surface and create controlled relative motion between the wheel and the ground. The visible outer surface consists of a P180 sanding belt, which has hook-and-loop strips attached to the inside in order to move it forward. The tensioning mechanism is continuously adjustable, using a simple threaded rod and nut. The motor transfers torque through a T-profile timing belt to a roller, which then drives the sanding belt. A metal support plate was placed underneath the contact area between the wheel and the belt. The purpose of the plate is to support the belt when exposed to pressure from the wheel and maintain a stable contact surface during operation.

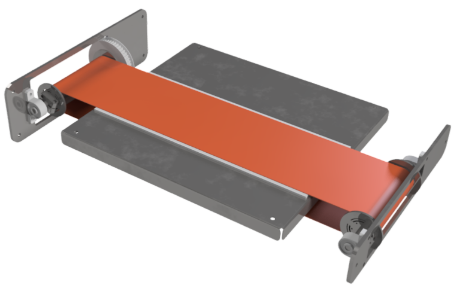

Figure 5.4: CAD model of the belt system

Both the wheel and the belt are powered by two identical motors. They are 12 V brushed DC motors with integrated planetary gears. As is, they are rated for 2 Nm of torque at 67 RPM. However, the two subsystems require totally different specifications, resulting in the addition of two different gearing systems. The wheel transmission consists of a three-stage gear train, resulting in a final speed of close to 1 RPM, enabling slow and controlled motion of the wheel. The belt uses a pulley system instead, achieving a reduction ratio of 3:1, meant to allow the wheel and belt to synchronise when the motors run at the same speeds.

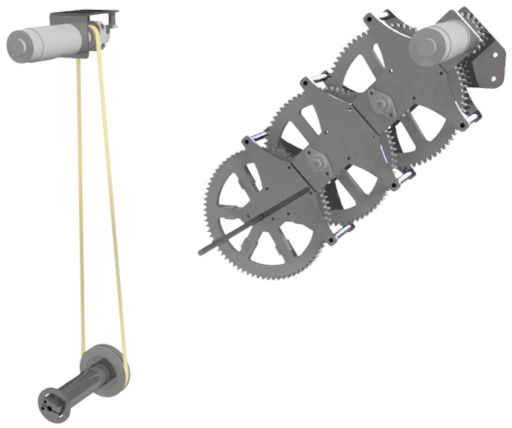

Figure 5.5: CAD model of the gearing systems

Slip is generated by controlling the speed difference between the wheel and the belt. When both move at the same speed, no slip occurs. When the speeds differ, slip is introduced at the contact surface, which affects the deformation of the bristles mounted on the wheel. Using this method, the system allows for controlled testing of different operating conditions and their effect on bristle behaviour.
The motion of the wheel and belt is controlled by an Arduino- based electrical system, which allows the system to control the two DC motors separately. This enables the relative speed between the wheel and belt to be regulated, creating controlled slip conditions during operation.

5.1.2 Safety

In the beginning of the project it was feared that the demonstrator might emit small fast travelling projectiles, similar to what can happen with tyres on real cars. This was later deemed a non-issue since the wheel operates at relatively low speeds.

Because the entire demonstrator is enclosed within the frame, it also serves as an indicator of a defined safety zone. Its box-shaped design provides a clear boundary of where the machine components begin and end, making it less ambiguous where it is safe to place hands during operation. All parts intended for interaction are separated from the main frame structure; the buttons are connected via extended wiring and the power supply is an external plug. The predominantly metal construction also contributes to reducing the risk of fire.

The conversion from 230 V mains (wall outlet) voltage is not only required for the electrical components to function, but also significantly reduces the risk of serious electrical injury. No exposed wires are present, as all of the electronics are enclosed in shrink wrap. This reduces the risk of both electric shock and fire and prevents entanglement with moving parts.

In order to prevent accidental cutting, the metal parts have had their sides lightly sanded down and the sound levels of the components were well below the recommended daily background noise.

5.1.3 Ergonomic systems

The box shape of the design allows for a familiar lift dynamic. However, the weight distribution is suboptimal, as the demonstrator does not have its centre of mass at the bottom. The imbalance is nevertheless small enough to avoid significant stability issues. The railings that make up the frame can also be used as handles for carrying.

5.1.4 Recycle-ability and environmental concern

In order to effectively recycle any given system in the demonstrator, it needs to be separated into groups of materials. With the current design, this process is streamlined, as very few parts are permanently attached to each other; most components are held together by screws that can be assembled and disassembled as needed.

The only metals used are aluminium and steel. Aluminium is highly suitable for recycling, with recycled aluminium requiring approximately 95% less energy compared to producing new material. For steel, this reduction is around 72% [11]. However, the components most likely to degrade in quality first are the bristles, since they are subjected to friction during operation. The TPU is recyclable, meaning that the bristles can be recycled [12].

5.1.5 Maintenance

The demonstrator is largely constructed from commercially available materials and components, combined with custom-designed mechanical parts. The bristles and spokes can be mounted, removed, and replaced as needed. Autodesk Inventor files and step files for most of the custom mechanical components are available upon request via the examiner or supervisor. It must be noted that not all CAD files fully match the current physical parts, since some minor changes have been made.

The majority of the demonstrator can be disassembled using screws, allowing individual parts to be easily removed and replaced. Very few components are permanently joined, which makes the system modular and simplifies maintenance.

5.2 Development of the demonstrator

This section describes the development and testing process that led to the final design described in section 5.1. Several concepts and manufacturing approaches were evaluated and iterated during the development phase. All this was done with the RS matrix in mind, ensuring that the majority of the requirements and desirables were fulfilled

5.2.1 Manufacturing considerations

There have been two main influences during the construction of the demonstrator: the limits imposed by available manufacturing equipment and the need for modularity.

The manufacturing of parts was carried out in the workshop *Prototyplabbet* at Chalmers. This imposed clear restrictions on the available manufacturing methods. Most of the equipment consisted of handheld tools or manually operated machinery, such as a pillar drill and a band saw. This affected achievable accuracy and tolerances, which in turn influenced how several components were designed and assembled. However, a water jet cutter and several 3D-printers were also available. Due to their higher precision, these were used to manufacture the majority of the parts. In addition, with the help of fellow students, some components were CNC-milled, allowing for improved fit and reduced risk of assembly issues.

When creating a one-off prototype, it is often more time-efficient to produce and test an initial version rather than ensuring that every detail works perfectly before manufacturing. This approach was used throughout the project. Only a limited number of parts had to be revised or remade due to incompatibility problems. This reduced the time spent on detailed CAD revisions while only slightly increasing manufacturing time. Most parts functioned either directly or after minor adjustments. As a result, the final prototype does not perfectly match all original CAD models.

Welding and glue were avoided to the greatest extent possible. This made almost every part interchangeable and easier to modify during assembly and testing. The main disadvantage of this approach was that it often required a larger number of individual components, making assembly more time consuming. However, the advantages outweighed this. Parts that did not fit perfectly could be adjusted more easily, and components could be replaced entirely when needed. This was especially important as several parts, such as the bristles and the spokes, were developed through an iterative process that required multiple design revisions.

Modularity was therefore an important design principle throughout the project. Many parts were designed to allow future modifications or alternative solutions to be tested. This made it possible to adapt and improve the demonstrator during development without requiring major redesigns.

5.2.2 Frame

Several frame ideas were considered in the early stages, including wood and various metals. As the design developed, it became clear that the frame needed to be both stiff and easy to adjust during testing.

Aluminium profiles were chosen, mainly for their relatively low weight and stable structure. This choice was directly linked to the RS, where low weight and easy transport were defined as important requirements. The profiles were connected using standardised corner joints, which simplified assembly while also improving structural rigidity. This contributed to reducing unwanted movement and vibrations during operation, improving the repeatability and visibility of the demonstrations. The rails in the frame allow for positional adjustment of both the wheel and the roller assemblies, making it possible to control the contact pressure between the wheel and the belt. This also simplifies assembly, maintenance, and component replacement.

In addition, the size restrictions defined in the RS influenced the final dimensions of the system. The total structure was therefore kept within $L + W + H = 2000$ mm to fulfil the requirement.

5.2.3 Bristles

In order for the demonstrator to function as an effective teaching tool, it was considered important that the deformation and slip be observable from a distance. The bristles were therefore designed with exaggerated dimensions, with a profile height of 30 mm, a profile width of 20 mm, a base thickness of 5 mm and spanning the full width (120 mm) of the wheel. If the wheel could achieve a 200 mm contact length with the belt, this would allow approximately six or seven bristles to be in contact with the ground at once, given a spacing distance of 10 mm between each bristle. All values were selected to achieve a balanced compromise between the relevant design considerations.

The development of the bristles went through several iterations before a suitable solution was achieved. Initially, the idea was to cut out the bristles in the foam rubber wheel and reinforce it with an external plastic armour. However, testing showed that the foam rubber was too soft, causing the bristles to compress almost completely under the load of the wheel. In addition, the proposed reinforcement methods were either permanent, which conflicted with the requirement that the bristles should be replaceable, or were considered impractical and unreliable.

A different approach was therefore investigated in which the bristles were manufactured separately using TPU through 3D-printing. This solution made the bristles fully replaceable and recyclable thus fulfilling the requirements set in the RS. It also enabled iteration of different geometries and stiffnesses. To determine a suitable design for the bristles, several test prints with different wall thicknesses were evaluated before a final decision was made.

The first bristle, shown in figure 5.6, featured a 2 mm thick, bendable structure with a thicker base for support and anchoring. The profile of the bristle aimed to produce clear deformation that could highlight and enhance the effects of the brush model. Using a simple rectangular shape was intended to keep the focus on the important aspects without drawing distraction. The part was printed on a Prusa MK4 with 100% infill and a 0.2 mm layer height.

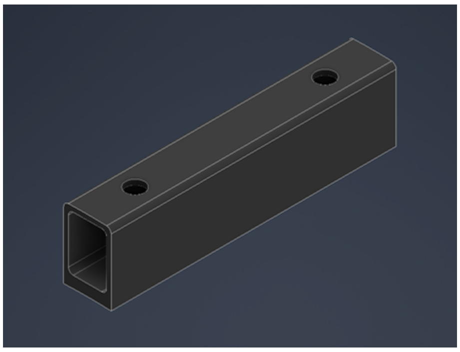

Figure 5.6: First bristle concept

The design was too stiff. Even more, there were also issues with the printer. To mitigate these issues, the second iteration was made 10 mm higher and wider, with thicker walls and printed with much lower infill, at around 10%.

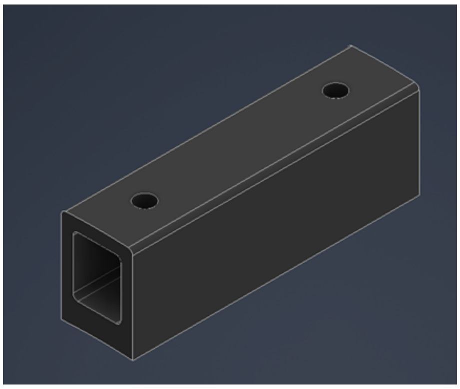

Figure 5.7: Second bristle concept

Despite these changes, the part was still too stiff. The next version therefore returned to the dimensions of the first iteration, but was instead modelled as a solid block with holes for screws. It was then printed at 5% infill.

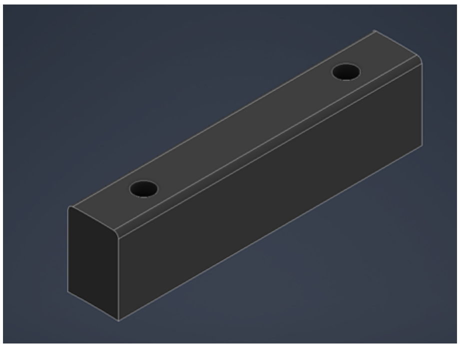

Figure 5.8: Third bristle concept

Straight out of the printer, the stiffness-issues remained. Cutting off the ends, though, revealed an internal structural X-pattern and a much less stiff part. Furthermore, cutting the X into pieces, ruining its structural integrity, created a part with much more promising results. The next print featured a design almost identical to the first one, but with a wall thickness of 1.2 mm instead of 2 mm.

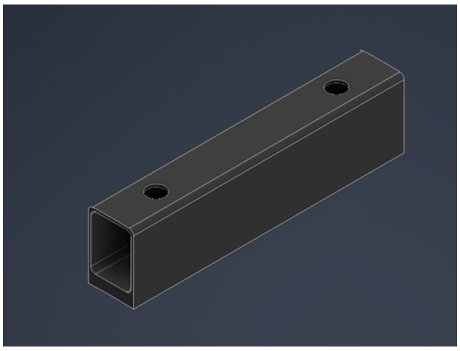

Figure 5.9: Final bristle concept

To evaluate this bristle concept, a simple test was performed to assess its deformation. The force required to create the desired contact length of 200 mm was estimated to be 60 N. This estimation was made using the plastic foam wheel, along with the aluminium sheet, mentioned in the next part of this chapter. The test was executed by pressing the components against a kitchen scale while measuring the contact length. Distributed over the six bristles thought to be in contact with the belt, this corresponds to approximately 10 N of normal force per bristle. Using the kitchen scale once again and pressing a bristle onto it at around 1 kg, the design showed a lot of potential when slid against the scale back and forth. It held up to the normal force while clearly showing tangential deformation and this bristle design was therefore chosen.

Needing to switch out the bristles due to wear from the belt would cause issues. The long printing time, combined with the nearly 100 screws required for mounting, results in significant maintenance time. A protective wearing surface, made from 3D-printed *Polyethylene Terephthalate Glycol* (PETG) was therefore made. They use a clip-in mechanism that reuses the through-holes for the screws on the bristles. Printing all 48 of them on the Snapmaker U1 can be done in around ten hours, split into two batches. Furthermore, the clip-in mechanism makes for very easy swaps.

5.2.4 Wheel

The wheel was designed as the central component of the system and was required to both maintain its overall shape and deform locally at the contact surface. This deformation is essential for visualising brush model behaviour, since it allows for multiple bristles to be in contact with the ground simultaneously. During the early prototyping phase, two alternative wheel concepts were investigated to identify the best solution.

Before selecting the final wheel structure, a central hub with side plates was designed and manufactured. This assembly was intended to support both wheel concepts considered during development and therefore allowed different solutions to be tested without redesigning the entire hub. Surrounding the wheel's inner structure, a cord of constant length was required to stay true to the theory. For this, a 0.5 mm thin aluminium sheet was selected.

The first concept to be tested was a solid wheel made from plastic foam. Since the available foam material was not thick enough, two sheets were glued together, resulting in a total thickness of approximately 110 mm to avoid buckling. However, the glue recommended for the material did not provide a strong enough bond, and there were concerns that the layers would separate under load. When the wheel was tested together with the outer aluminium sheet, it was also found that the material deformed in an uncontrolled way, especially sideways, which was not desired. In addition, it was unclear how the wheel could be reliably attached to the axle, since glue alone was not considered a suitable solution for transferring torque. Because of these problems, this idea was discarded.

After this, a new idea was developed using 3D-printed spokes made of TPU (95A). The idea of flexible TPU spokes was a derivative of the meta-material concept. The large 3D-printers that could have printed an entire wheel with metamaterial structures are quite unreliable. Furthermore, TPU is a problematic filament to print with, easily causing jamming and other issues. Dividing it into several printable pieces reduces the risks and severity of a failed print. It also essentially turns it into a typical spoke-style wheel.

Just like the bristles, the spokes had an iterative development process. Moreover, because the spokes were designed after the bristles, it made sense to reuse the same mounting mechanism for both parts. In the other end of the spokes, a joint was added, allowing for easy installation in a tighter space, as well as adding more flexibility to the structure. The first iteration, seen in figure 5.10, consisted of two simple mounting bases, with a curved 2 mm thick plate tying them together. Making the plate curved makes the bend predictable, so the spokes do not interfere with each other.

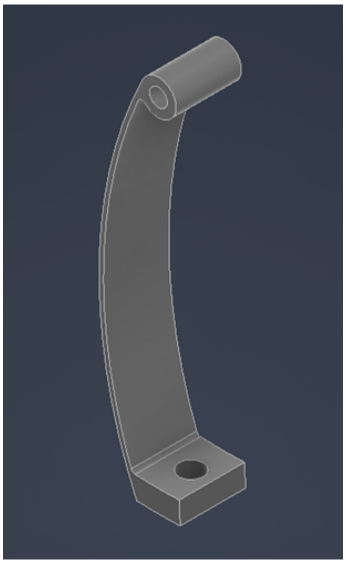

Figure 5.10: First spoke concept

The following two iterations featured an identical design, with the only difference being that the bent plate grew 1 mm thicker for each version. The fourth iteration, however, featured more changes. It kept the 4 mm thick plate but attached to the mounting bases in new ways. For the joint, the location was moved to decrease interference between spokes. A curve was added to the outwards base, with the purpose of mitigating rotation in the outwards end.

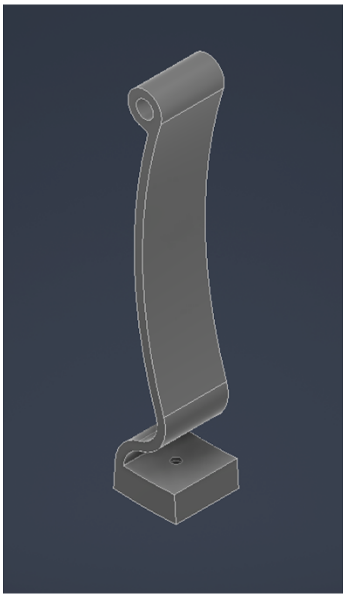

Figure 5.11: Fourth spoke concept

The S-bend did not work as intended, so in the final design, this idea was discarded. The final design also featured slimmed down mounting bases to reduce printing times. The spokes were printed on the same printers and with the same settings as the bristles.

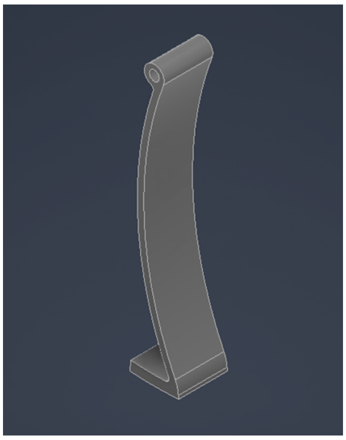

Figure 5.12: Final spoke concept

The initial idea was to have parallel spokes to improve lateral stiffness. However, due to printing time limitations, a prototype with only a single row of spokes in the centre of the wheel was tested first. This solution proved to provide both good elasticity and very limited lateral movement, making additional spoke rows unnecessary.

To position the spokes correctly, spacers were designed and 3D-printed using PETG and added to the threaded rods in the hub assembly. This ensured that the spokes remained centred within the wheel. The combination of the central hub, the spokes, spacers, and outer aluminium ring resulted in a wheel that balances rigidity and controlled deformation very well.

5.2.5 Belt system

To achieve the desired interaction with the wheel, a moving contact surface needed to be supported and driven in a reliable way. The initial idea was to have rollers directly connected to a wide, flat belt, driving it through pure friction, with a metal plane underneath acting as support. However, after assumptions regarding the friction forces applied, it was reasoned that the contact between the moving belt and the rollers would most likely not withstand these forces without slipping. The next idea was to have one timing belts on each side of the flat belt, but that concept was quickly discarded as a single central timing belt would have been sufficient.

The next problem to solve was the tensioning of the belt. One solution was to use a tensioner pulley that would sit under the belt and push it up, generating tension. Another idea was to use a spring mechanism that would attach to the roller and add constant tension. However, both of these solutions were time intensive, and in the end, a simple screw lock mechanism was used.

The P180 sanding belt was chosen as the flat belt because it is designed to withstand high friction and shear forces during operation in sanding machines. It was therefore considered suitable for handling the stresses generated in the demonstrator. Its availability on the market, as well as its relatively low cost, also contributed to its selection. For the timing belt, a T-profiled belt was selected, as it is well suited for general-purpose drives with moderate load requirements, while more advanced profiles such as AT are intended for higher load capacity [13].

Attaching the sanding belt to the timing belt also proved to be a challenge. Initially, the idea was to rough up the top of the timing belt and glue it to the sanding belt, but this required the glue to both bind to Polyurethane and be flexible enough to handle the bending motion required when passing through the rollers. After discussing the matter with foremen at Beijer and professionals from Sika, it became clear that the problem was very unique and there was no real way of knowing if the glue and adhesive at their disposal would work or not. The first test was therefore conducted using the least damaging method: double-sided tape.

Although the construction had many upsides, it had a disastrous downside that was uncovered when it was supposed to be assembled. Consider figure 5.13, of the two lines. In this case, they represent the timing belt and the sanding belt. Taping or glueing them together works; however, when bent around the rollers, as shown in figure 5.14, the outer layer (sanding belt) needs to travel a further distance than the inner layer (timing belt), requiring it to stretch. Neither the timing belt nor the sanding belt is particularly stretchable, resulting in high sheer tresses between the layers. In turn, this resulted in the two components being released from each other.

Figure 5.13: Belt system in flat configuration

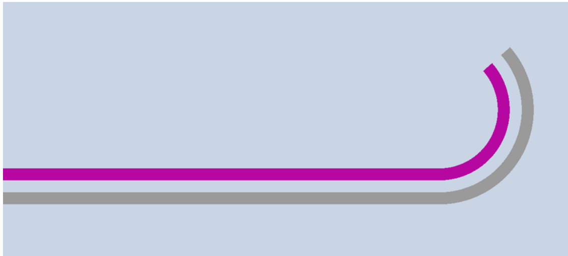

Figure 5.14: Bending of belt system, causing mismatch in layer travel distance

The issue occurred at an inopportune time, creating the need for a quick solution. After brainstorming in pairs, there were a handful of solutions deemed potentially viable. Most consisted of making the rollers sticky and relying on tension to keep the sandpaper moving. The cheapest and quickest solution to test was the use of hook-and-loop fasteners. Hook-and-loop fasteners have great reusability, and the rollers naturally detach while rotating the belt forward. It minimises slip between the rollers and the belt, moving it steadily forward due to its strong resistance to shear forces. These fasteners were therefore implemented in the final demonstrator.

5.2.6 Drive system

The motor was chosen based on an estimation of the required torque to overcome friction between the wheel and the contact surface. To approximate this, a simple test was performed in which the plastic foam wheel was pressed against a surface to achieve a contact length of approximately 200 mm, while the normal force was measured using a scale. The normal force was measured to be approximately 60 N. The coefficient of friction was estimated based on typical material pairings.

The required torque was then calculated using $T = \mu \cdot N \cdot r$ where μ is the coefficient of friction, N is the normal force, and r is the wheel radius. With a wheel radius of 0.25 m and an assumed relatively high friction coefficient of 1, the resulting torque was estimated to be approximately 15 Nm. As the friction coefficient was not directly measured and is subject to uncertainty, a conservative estimate was used.

The motor selected was a 12 V brushed DC motor and provided an output speed of approximately 67 rpm and a rated torque of 2 Nm. Although the motor itself provided some speed reduction through its internal gearbox, the output speed and torque were not sufficient for this application. To achieve the torque requirement and the desired low rotational speed of approximately 1 rpm with the selected motor, a gear reduction system was designed.

The motor was not chosen as the most optimal solution, but rather as a practical choice due to time constraints and limited availability of alternative options. For the belt drive system, the same motor type was used. The requirements for the belt system were lower than for the wheel system, especially in terms of torque, which made this choice acceptable. Using the same motor for both the belt system and the wheel system simplified the electrical design.

5.2.7 Gearing system

Determining an appropriate speed for the wheel was one of the most integral decisions of the project. Considering it is the first of its kind , knowing what is suitable beforehand can be difficult. It was not something that could be decided right away but had to wait until the plastic foam wheel was cut out, which served as a reference. The group decided that a bristle needed around 5-10 seconds to move along the 200 mm contact surface with the belt. Taking the mean value of 7.5 seconds resulted in around 1 RPM for the 500 mm wheel.

To have margins and not have the motor run at full speed constantly, the gearing was calculated for an output speed of 50 RPM instead of 67 RPM. To keep gear size down, a three-step gear was required, and for simplicity, three equal steps were used. Three 20T to 74T steps result in a reduction ratio of around 50.7:1. The module for the gear was dimensioned with the help of ChatGPT[9], which recommended a modulus of 1.5-2. However, for the sake of extending the gear to allow the motor to sit parallel with the wheel, the gears were ultimately made with a modulus of 2.5. Cutting gears with a water jet made it easy to add lightening holes to reduce efficiency losses. Nevertheless, the efficiency of the gearing system is expected to be low due to cheap ball bearings, pre-made shafts, and poor gear design.

Due to the difference in diameter between the wheel and the rollers, the two motors require massively different gearing systems. To keep the motor for the rollers out of the way, a simple one-step pulley-system was used. With a 16T driver pulley and a 48T driven pulley, the reduction ratio is 3:1, which is the correct ratio to synchronise speeds with the wheel. The pulleys are 3D-printed using PETG with 40% infill and a 0.08 mm layer height. These were only supposed to be used to test the concept; however, in testing, they worked well enough that they were left in the final product. This is something that most likely affects both efficiency and longevity negatively, so an upgrade to metal parts would be preferred.

5.2.8 Electrical design

The electrical system was designed to power, control, and monitor the motion of the wheel and belt. The system is supplied from a standard 230 V wall outlet, which is converted to 12 V DC using an AC-DC power supply. This voltage is compatible with the selected brushed DC motors, motor drivers, and control electronics.

An Arduino system was used to control the two motors separately. Since the Arduino cannot supply the required motor current directly, motor drivers were used as an interface between the Arduino and the motors. The signals originate from the Arduino and give commands to the motor drivers which in turn signal the DC motors. Separate control of the wheel and belt motors allows the relative speed between them to be regulated. This enables controlled slip conditions to be created during operation, which is necessary for observing bristle deformation.

Infrared sensors (IR) were used to monitor the rotational speed both for the wheel and the belt. The sensors detect changes in reflected light from rotating black and white disks. The disks are 3D-printed using PETG. The wheel has 20 black and 20 white zones mounted on the first large gear in the gearing system. The belt has 18 white and black zones and the disk is mounted right to the roller. These signals are read by the Arduino and used to estimate the rotational speeds.

The code for the Arduino was created with the help of ChatGPT. It calculates the speeds for the two systems by measuring the time it takes for the IR sensors to see the same colour twice. In practice, this means that one white zone and one black zone have passed the sensor. By taking the number of zones for each system, an angular speed can be calculated. When finalizing the RPM calculations, gearing for the wheel is also considered.

With known RPM values, PID-regulators were implemented to set speeds for the systems. At “idle” (correlation = 1), the speeds of the two systems are synchronised in a manner that gives the wheel and the belt the same tangential speed. The wheel is always set to a fixed 1 RPM, while the speed of the belt changes based on the desired speed correlation. To change correlation, two buttons are used; they increase or decrease the speed correlation by five percentile units at a time. The code used can be found in Appendix 3.

The detailed wiring of the motor drivers, sensors, buttons, and power supply is shown in Figure 5.15 and Figure 5.16 below. The motor drivers are connected to the Arduino using PWM signals, where the wheel motor driver was controlled through digital pin 9 and the belt motor driver through digital pin 5. The IR sensors were connected to digital pins 2 and 3, while two buttons connected to digital pins 8 and 4 were used to adjust the speed correlation.

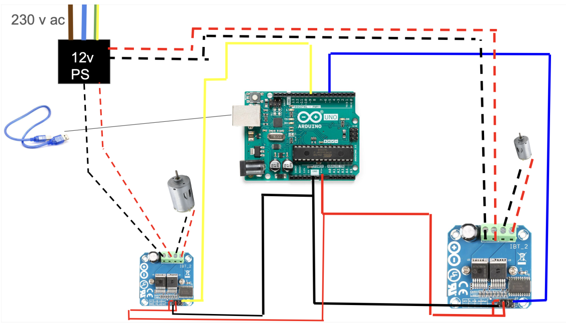

Figure 5.15: Electrical schematic for the Arduino with motors and motor drivers

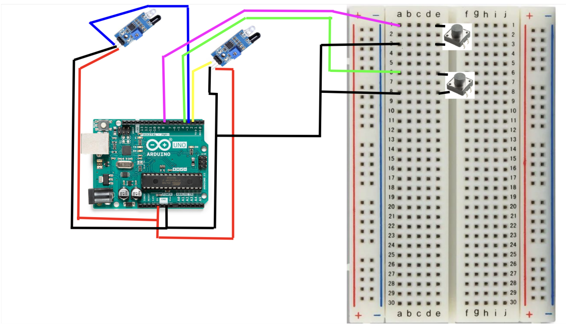

Figure 5.16: Electrical schematic for the Arduino with IR-sensors and buttons

5.3 Results

The testing of the demonstrator was done by changing the targeted correlation value by ten percentile units at a time, pausing in between to allow for the machine to stabilize. The maximum tested correlation was 1.7, while the minimum tested correlation was 0.6. The results are presented using simplified pictures. The figures are intended to illustrate the average state of a row of bristles along the contact length for a wheel rotating clockwise

At idle the deformation in the bristles is symmetric along the contact length, as seen in Fig. 5.17. When a bristle has travelled to the middle it stands straight, while the rest of them bend outwards.

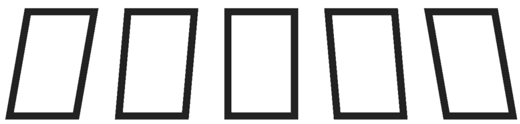

Figure 5.17: Bristle deformation at idle

Increasing the speed correlation, ranging from 1.1 to 1.3, there is a slight change in the pattern as seen in Fig. 5.18. Throughout the range, the pattern is quite similar, only making the bristles deform slightly more at higher correlations. The initial deformation when entering is almost entirely gone, shifting the straight bristle towards the leading edge.

Figure 5.18: Deformation at speed correlations 1.1 - 1.3

In the range of 1.4 to 1.8, seen in Fig. 5.19 the deformation becomes much more visible. The bristles have all started leaning the same way. When entering the contact-zone, the bristles catch onto the belt rather quickly. Towards the centre of the contact-zone, they straighten out a bit, before they return to bending even more than before. Furthermore, at the higher end of the range, the deformation is significantly larger than for the lower end.

Figure 5.19: Deformation at speed correlations 1.4 - 1.8

For correlation values below 1, the reduction in speed of the belt results in mostly similar behaviour as when speeding up, although reversed. At a speed correlation of around 0.9, the bristles deform like in Fig. 5.20. In the same manner, Fig. 5.21 represents the range from 0.8 to 0.7. There were mainly two observable differences in behaviour when speeding up and slowing down: The speed difference required to achieve the same amount of bending in the bristles was much lesser when slowing down than when speeding up the belt. The other difference was that the wheel was able to fully lose traction with the belt when slowing down. The behaviour was first observed at a speed correlation of around 0.7, oscillating between grip and no grip. Decreasing the correlation further, to 0.6, resulted in almost more slipping than sticking.

Figure 5.20: Deformation at a speed correlation of 0.9

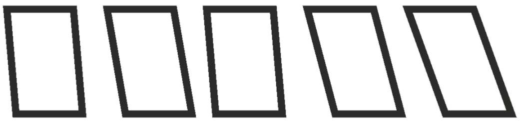

Figure 5.21: Deformation at speed correlations 0.8 - 0.7

5.4 Requirement fulfilment

To evaluate the final demonstrator, the completed design was assessed against the requirement specification matrix. Each requirement and desired criterion was reviewed based on testing, measurements, and observations to determine whether it had been fulfilled.

Several required and desired criteria were not fulfilled. Notably, the production cost exceeded the budget, certain safety concerns regarding pinch hazards remain unsolved, and visibility of the slip zone was only partially achieved. These shortcomings, together with the limitations in brush behaviour described in section 6.1, indicate that the demonstrator in its current form requires further development.

Table 5.1: Evaluation of requirement specification

No.	Criteria	Goal	R/D	Result	Status
Functions					
	Physically Visualise Brush Model		R	Partially achieved	Part. fulfilled
	Simulate Longitudinal Motion		R	Achieved	Fulfilled
	Simulate Lateral Motion		D	Not implemented	Not fulfilled
	Simulate Camber		D	Not implemented	Not fulfilled
	Collect & Compare w. Theory	Val. var. 10%	D	Not implemented	Not fulfilled
1. Performance					
1.1	Consistent slip relation	Var. 5%	D	Achieved	Fulfilled
1.2	Clearly Visible Deformation	From 3 m	R	Achieved	Fulfilled
1.3	Clearly Visible Deformation	From 5 m	D	Not achieved	Not fulfilled
1.4	Clearly Visible Slip Zone	From 3 m	D	Partially achieved	Part. fulfilled
1.5	Clearly Visible Slip Zone	From 5 m	D	Not achieved	Not fulfilled
2. Environment					
2.1	Env. Temperature	15–30 °C	R	Achieved	Fulfilled
3. Size					
3.1	Maximum L+W+H	2 m	R	1.6 m	Fulfilled
3.2	Maximum L+W+H	1.5 m	D	1.6 m	Not fulfilled
4. Mass					
4.1	Max weight	25 kg	R	22.5 kg	Fulfilled
4.2	Max weight	15 kg	D	22.5 kg	Not fulfilled
5. Ergonomics					
5.1	Maximum sound level	50 dB	D	60 dB	Not fulfilled
6. Safety					
6.1	Maximum sound level	80 dB	R	60 dB	Fulfilled
6.2	Min. Projectile Debris		R	Partially achieved	Part. fulfilled
6.3	Min. Risk of Fire		R	Achieved	Fulfilled
6.4	Min. Risk of Elec. Shocks		R	Achieved	Fulfilled
6.5	No Sharp Edges		R	Achieved	Fulfilled
6.6	Min. Risk of Burns		R	Achieved	Fulfilled
6.7	Min. Pinch Hazard		R	Not achieved	Not fulfilled
7. Material					
7.1	Bristles with Elastic Properties		R	Achieved	Fulfilled
8. Production Cost					
8.1	Maximum cost	10 000 kr	D	13 500 kr	Not fulfilled
9. Maintenance					
9.1	Replaceable Brush	≤30 min	R	Achieved	Fulfilled
9.2	Easily Replaceable Brush	≤10 min	D	Achieved	Fulfilled
10. Reuse and Recycle					
10.1	Easily Repairable		D	Achieved	Fulfilled
10.2	Recyclable Bristles		D	Achieved	Fulfilled

6

Conclusion

The conclusion houses discussions regarding the results, as well as practical and useful information concerning future development.

6.1 Discussion

During testing, the cord took a slight but obvious “w-shape” along the contact zone, see Fig. 6.1. The shape became more prominent for speed correlations further from idle. The cause of this phenomena remains unclear. Initially, it was attributed to an incorrect force distribution, as a result of the design of the spokes. When the wheel is compressed, the spokes bend a lot. This could result in collapsed spokes that can no longer apply sufficient pressure. Furthermore, the spokes are fixed in the aluminium cord, most likely resulting in significant torque contributions that may be unwanted.

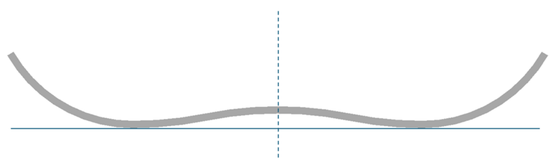

Figure 6.1: W-shaped cord

To test these theories, a couple of simple tests were performed. A loose spoke was compressed by hand, and although it was bent further than in the demonstrator, it did not seem to collapse. Additionally, a similar "hands-on" test was performed on the system in its entirety. The bristles in contact with the contact surface were lifted upwards by hand, one by one. When doing this, it seemed that the bristles in the centre of the contact surface required more force to lift than the ones further from the centre. These tests indicate that the static force distribution is correct according to the theory, although further testing is necessary in order to verify it.

The simple test that was performed to check whether or not the force distribution is correct was done without the wheel turning. This means that the torque contributions from the motors where not taken into account. Differences between static and dynamic force distribution could be the reason for the observed w-shape. The addition of torque from the wheel may concentrate larger forces at the deflection point (the point on the contact surface where the wheel first makes contact), essentially creating an inverse force distribution.

The final, and most likely reason for the phenomena is that the aluminium plastically buckles, as it enters the deflection point. The buckling is slight enough that the wheel mostly keeps its circular shape, but when looking closely, there are several points around the wheel at witch it has buckled. At first, the phenomena was only seen at speed correlations much further from idle, however, after running the demonstrator for a while, the w-shape got more noticeable at all correlations. This would be explained by plastic buckling at speed correlations further from idle, still being visible when going back to idle.

The most interesting phenomenon observed was at idle. In theory, the speed along the contact surface should be constant, however, it is only at the centre that the bristles stand straight. The reason for this is unclear. One contributing factor could be that a lot of bending occurs as the bristles enter the contact zone. Because the bristles have been made into rectangles, essentially connecting what could have been separate bristles, the "second" bristle to enter the contact zone becomes pre-deformed. This deformation happens when the bristle is still in the air, decreasing its resistance against bending while loading it with the same amount of force as when it is pressed against the contact zone fully.

There were observations regarding discrepancies in brush deformation. There are several contributing factors to this. The holes in the aluminium cord are drilled by hand, making the placement of the bristles vary slightly. This means that they are not perfectly square with each other, which results in uneven force distribution. Furthermore, a few bristles have been manufactured using another printer model, as well as using older filament that had absorbed more moisture. Finally, TPU is viscoelastic, meaning that after a couple of rounds it may start to inherit the bent shape, and become "pre-bent". As a result, when using the demonstrator, a single bristle cannot be studied, but it must instead be viewed as a whole, sorting out behaviour that do not match what is expected.

6.1.1 Translation of the brush model into a real-world system

The first research question concerns how the assumptions and mechanisms of the brush model can be translated into a mechanical design suitable for a real-world demonstrator.

The deformation in the contact area is represented by flexible 3D-printed bristles, made from TPU, and mounted on the wheel. These bristles act as a physical representation of the brush elements in the model and make it possible to observe how deformation develops during operation. The slip behaviour in the theoretical model is represented by creating relative motion between two separately driven parts: the wheel and the belt (road surface). This allows different speed differences to be set, which correspond to different slip conditions in the model. The aluminium cord helps maintain the constant wheel circumference reflecting the theoretical assumptions of the brush model. These three features represent the key elements of the brush model.

However, for a successful visualisation of the brush model, pausing it at any moment should give a similar picture as in Fig. 6.2. Thus, the demonstrator cannot visualise the model. The bristles fail to continuously increase their deformation along the contact zone. Instead, they straighten out toward the middle of the contact zone, creating an abrupt interruption in the expected deformation pattern.

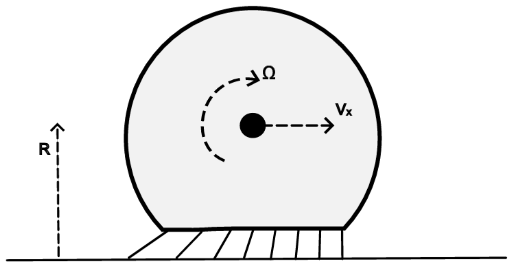

Figure 6.2: Desired bristle behaviour. Drawn without a sliding zone

Although the demonstrator is unable to visualize the brush model in its entirety, there are elements of the brush model that can be observed by using the demonstrator. The bristles deform increasingly more for speed correlations further from idle, regardless of whether the speed of the belt is increased or decreased. When moving along the contact zone, they deform increasingly more, besides when they approach the centre. Although the slip-zone was not distinctly present, similar dynamics could be observed while the entire wheel slipped.

It can therefore be concluded that a wheel-road type setup with controllable motion and visible bristle deformation is a viable approach for translating the brush model into a real-world demonstrator. However, the current implementation does not fully succeed in this translation and further design iterations are needed before the demonstrator can reliably represent the brush model.

6.1.2 Limitations compared to the theoretical model

The second research question concerns what limitations the real-world demonstrator has compared to the theoretical brush model. The demonstrator is mainly designed to visually demonstrate deformation and stick-slip, so the most relevant comparison is how well these behaviours are represented.

One limitation is related to material behaviour. The theoretical model assumes simplified and idealised elastic behaviour of the bristles, where deformation changes proportionally with the applied load. The TPU material used in the demonstrator does not behave perfectly linearly, meaning that its stiffness may vary depending on the amount of deformation. This means that the physical deformation is not an exact match to the theoretical model. However, this does not have a major impact on the purpose of the demonstrator, since the main goal is to visually show deformation and not to reproduce the exact theoretical material behaviour.

Another limitation is that the demonstrator only represents longitudinal behaviour. The theoretical brush model can also include lateral effects such as slip angle and camber. These effects are not included in the current design since the focus has been on showing bristle behaviour in one direction.

In addition, the theoretical model describes the contact behaviour in a more detailed and continuous way. In the demonstrator, this is simplified since only a limited number of discrete bristles are used, and the behaviour can only be observed visually during operation. This means that the contact behaviour cannot be measured or analysed in the same way as in the theoretical model, which limits comparison between the two.

It can therefore be concluded that the demonstrator is a simplified version of the brush model. It does not include all aspects of the theory, but it still captures the most important behaviours, including bristle deformation and aspects of slip behaviour, such as traction loss at low speed correlations.

6.2 Future development

Given that the demonstrator does not yet fully achieve its intended educational purpose, future development should be prioritised. The modularity of the product does facilitate modifications, and there are several improvements that could address the identified shortcomings. The most urgent of these concerns is the w-shape, the bristle design and the clarity of the stick-slip visualisation.

6.2.1 Idea discussion for possible correction of the w-shape

To gain better understanding of why the w-shape appears, a few simple preliminary tests are recommended. By moving the contact surface, the belt and its gearing system downwards, the demonstrator can be tested at a lower contact pressure. On the contrary, by moving the wheel and its gearing system downwards, the demonstrator can be tested at a higher contact pressure. As a next step, the bristles should be exchanged for a weaker version, that deforms more easily. Running the demonstrator in these different configurations should hopefully garner more information regarding the phenomena.

If the underlying cause cannot be determined based on the results from these tests, more comprehensive practical testing is the recommended next step. To determine if continuos plastic buckling of the aluminium cord is the root issue, it should be replaced with a material that is less susceptible to plastic buckling under the tested conditions. The preferred material for this test is 0.2 mm sheet steel. Should this prove unsuitable, a 2 mm thick *Ethylene Propylene Diene Monomer* (EPDM) sheet is recommended as an alternative.

Failing to establish the underlying cause after these tests, the proposed action is to measure the contact pressure at different points of the contact zone. The data will give a definitive answer to whether the demonstrator replicates the force distribution of the brush model; preferably, this should be done both in static and when the demonstrator is running.

A different approach could be to focus on how the brush model can be demonstrated, without concern for why the w-shape appears. An idea for correcting the shape was to apply a permanent force to the point of the protrusion, in addition to the radial force from the spokes in the middle of the contact zone. This solution would flatten the aluminium cord, making it parallel with the contact surface; it would ensure steady contact between the bristles and the belt, throughout the entire contact zone. The main problem with this solution is, as stated earlier, that it does not address the root cause of the issue, but instead compensates for its effects. It results in an unnecessarily complicated construction, and because the root issue has not been resolved, other related issues may arise.

6.2.2 Future improvements for the bristles

The bristles have a lot of potential for improvement. Different shapes, materials, and thicknesses could all be used to create something that can fully visualise the brush model. The use of metamaterial structures in the bristles could also be further explored. By designing the internal structure of the bristles, it would be possible to tune their deformation behaviour. This could make it easier to achieve a controlled and repeatable response under load. Regarding the ease of changing bristles, there is an issue when it comes to printing times. Each bristle takes roughly two and a half hours to print; swapping out 48 of them requires a lot of time. Adding some kind of wearing surface to the bottom of the "bristles" could eliminate the need to change them out entirely. Perhaps some sort of EPDM sealing strip could replace the 3D-printed bristles, reducing the production time significantly. Adding blind rivet nuts could ease the installation of bristles a lot; however, when mounting them, they destroy the thin metal sheet, making it a poor choice. Perhaps different mounting methods could make it a viable upgrade. They are very accessible though, since there is just one row of spokes.

It would also be valuable to include bending sensors in the bristles. This would make it possible to measure how much the bristles deform during operation instead of only observing it visually. By collecting data about speed and brush deformation, it would be possible to relate the measurements to the theoretical model. Combining the sensor data with the theory could help improve the understanding of the tyre brush model. The addition of a digital screen could display this data in real time. Not only that, but it would be a helpful tool in displaying current settings of speed and potential future parameters that get added. Following the same trajectory, an LED indicator strip could be an informative and pedagogical supplement in showcasing the slip-zone.

Being able to adjust the ground-pressure could help increase or decrease the effects of the model to the desired amount. As of now it is possible, although it does require loosening four screws and manually adjusting the height of the wheel. Being able to automatically adjust the ground-pressure could help simulate acceleration, different speeds and the magnitude of deformation in the bristles.

6.2.3 Unimplemented features

Due to time and budget constraints, there were lots of minor ideas that could not be implemented or added. The simple things include adding a kill switch, protecting the parts from rust using clear-coat and adding acrylic panels to all sides of the product. At the moment, moving parts such as the wheel and the belt are exposed. This may pose a risk during operation. By adding a protective enclosure, for example using transparent materials such as acrylic, the user could be protected from moving components while still being able to observe the system. Furthermore, wheels could be added to the bottom of the machine for easier movement, and handles should be attached on each short side for carrying short distances.

An important improvement is to include lateral forces in addition to the current focus on longitudinal forces. Lateral forces could be introduced by allowing the wheel to be rotated relative to the direction of motion, creating a slip angle. This would result in lateral deformation of the bristles and would make it possible to study side forces. It would also allow the system to demonstrate a combination of longitudinal and lateral forces, making the behaviour more realistic. Bristles must then be redesigned so that they can bend in the lateral direction. To be able to show combined slip, the bristles have to allow for both lateral and longitudinal deformation simultaneously.

Another possible improvement is to introduce an adjustable camber angle. In the current design, the camber angle is fixed at zero, which limits the range of conditions that can be studied. By adding a mechanism to control the tilt of the wheel, it would be possible to investigate how the contact area and brush deformation change with different camber angles.

However, attempting to add either the turning feature or camber possibility would require a lot of rework. To get a wheel that behaves more appropriately in these scenarios, it would likely require two weaker parallel spokes rather than the stronger centre spoke in the current configuration. Moreover, both gearing solutions would cause issues. Using other motors with more appropriate gearing that do not require additional gearing would make for a cleaner, more reliable solution. Another big advantage would be weight reduction. Nevertheless, the current solution has one advantage; it reduces the depth of the product, as the motors can sit parallel to the wheel and the belt. Achieving the same product size would otherwise require worm gears, which limit the available selection.

Bibliography

[1] B. Jacobson et al. *Vehicle Motion Engineering*, Chalmers University of Technology, Gothenburg, Sweden, 2026. [Online] Available: https://research.chalmers.se/publication/548872/file/548872_Fulltext.pdf. [Accessed: Apr. 8, 2026].

[2] H. B. Pacejka, *Tyre and Vehicle Dynamics*, 2nd ed. Oxford, U.K.: Butterworth-Heinemann, 2006.

[3] Chalmers University of Technology, “Requirement specification matrix template,” course material for MMF176, Canvas, [Accessed: May. 13, 2026].

[4] Delft University of Technology, “Morphological Chart,” Delft Design Guide. [Online]. Available: https://arl.human.cornell.edu/PAGES_Delft/Morpholigical_Chart-deeper.pdf

[5] Chalmers University of Technology, “Elimination matrix template,” course material for MMF176, Canvas, [Accessed: May. 13, 2026].

[6] Hasso Plattner Institute, "Metamaterial Mechanisms", [Online]. Available: https://hpi.de/baudisch/projects/metamaterial-mechanisms.html. [Accessed: Apr. 8, 2026].

[7] Adidas, "What is 4DFWD?," Adidas Blog, 2022. [Online]. Available: https://www.adidas.com/us/blog/680801-what-is-4dfwd?msockid=250ead2b22ec62c61608be7423c463d0. [Accessed: Apr. 20, 2026]

[8] Princeton Engineering, "Material? Robot? It’s a metabot," Apr. 23, 2025. [Online]. Available: https://engineering.princeton.edu/news/2025/04/23/material-robot-its-metabot. [Accessed: Apr. 8, 2026].

[9] OpenAI, "ChatGPT," [Online]. Available: https://chatgpt.com/. [Accessed: Apr. 8, 2026].

[10] J. Martinsson Bonde, "Morpheus - Morphological Matrix Tool," [Online]. Available: https://morpheus.martinsson-bonde.com/. [Accessed: Apr. 8, 2026].

[11] EURIC, "Metal Recycling Factsheet," Circular Economy Platform. [Online]. Available: https://circulareconomy.europa.eu/platform/sites/default/files/euric_metal_recycling_factsheet.pdf. [Accessed: May 12, 2026].

[12] Recycling Today, “TPU Recycling Shredding and Pelletizing”. [Online]. Available: https://www.recyclingtoday.org/blogs/news/tpu-recycling-shredding-and-pelletizing. [Accessed: May 12, 2026].

[13] York Industries, "Understanding Belt Profiles: PowerGrip GT2, GT3, HTD, MXL, XL, L, 40 DP, A and AT," 2025. [Online]. Available: https://www.york-ind.com/blog/timing-belts/

understanding-belt-profiles-powergrip-gt2-gt3-htd-mxl-xl-l-40-dp-a-and-at. [Accessed: Apr. 21, 2026]

[14] Arbetsmiljöverket, “Risker i arbetsmiljön (AFS 2023:10),” 2023. [Online]. Available: https://www.av.se/arbetsmiljoarbete-och-inspektioner/publikationer/foreskrifter/afs-202310/. [Accessed: May 12, 2026].

A

Appendix 1

Generate Longitudinal Motion	Belt (Granta material)	Brainstorm
	Pulley-system	Brainstorm
	Individual motors (bristles)	Brainstorm
	Fluid movement	Brainstorm
	Mechanical pushing	Brainstorm
	Rotating plate	AI
	Multiple rollers as surface	AI
	Magnet	Existing
	Electromagnet	Existing
Simulate Camber	Manual fixed rotation (degree indexing)	Brainstorm
	Motorized angling	Brainstorm
	Pneumatic angling	AI
Generate Lateral Motion	Belt (Granta material)	Brainstorm
	Pulley-system	Brainstorm
	Individual motors (brush strands)	Brainstorm
	Fluid movement	Brainstorm
	Mechanical pushing	Brainstorm
	Rotating plate	AI
	Multiple rollers as surface	AI
	Magnet	Existing
	Electromagnet	Existing
Simulate Road Contact	Flexible material (Granta)	Brainstorm
	Brush belt	Brainstorm
	Rotating hexagon	Brainstorm
	Pneumatic loading system	AI
	Loading by belt tension	AI
	Oil cylinder	AI
	Magnets	Existing
Displaceable Brush Geometry	Flexible chopped material	Brainstorm
	Flexible transparent material	Brainstorm
	Springs	Brainstorm
	Pulleys	Brainstorm
	Air cushion bristles	AI
	Torsion rods	AI
	Magnet	Existing
	Electromagnet	Existing
	Metamaterial	Existing
Regulate Motion	Power regulator	Brainstorm
	Gearbox	Brainstorm
	Hand operated	Brainstorm
Support Structure	Metal frame	Brainstorm
	Wooden frame	Brainstorm

	3D-printed chassis	Brainstorm
	Harness	Brainstorm
Protect User	Plexiglas wall	Brainstorm
	Gloves / glasses / earmuffs	Brainstorm
	Automatic failsafe	Brainstorm
	Emergency stop button	Brainstorm
	Safety net	Brainstorm
	Instructions	Brainstorm
Supply Energy	Battery	Brainstorm
	Diesel generator	Brainstorm
	Solar panels	Brainstorm
	Hand operated	Brainstorm
	Wall outlet	Brainstorm
Receive User Input	Button	Brainstorm
	Lever	Brainstorm
	Hand operated	Brainstorm
	Voice operated	Brainstorm
	Dial	Brainstorm
Collect Data	Pressure sensor	Brainstorm
	Motion sensor	Brainstorm
	Camera	Brainstorm
	Ampere meter	Brainstorm
	Ruler (manual)	Brainstorm
	Flex sensor	Existing
Display Brush Deformation	Light magnification	Brainstorm
	Strobe light	Brainstorm
	Camera	Brainstorm
	Visually clear material	Brainstorm
Display Slip	LED slip indicator	AI
	Color changing contact film	AI
	Sound indicator	AI
Process Data	Arduino	Brainstorm
	Raspberry Pi	Brainstorm
	Laptop	Brainstorm
	Paper & pencil	Brainstorm

Figure A.1: All generated ideas (section 4.1.3)

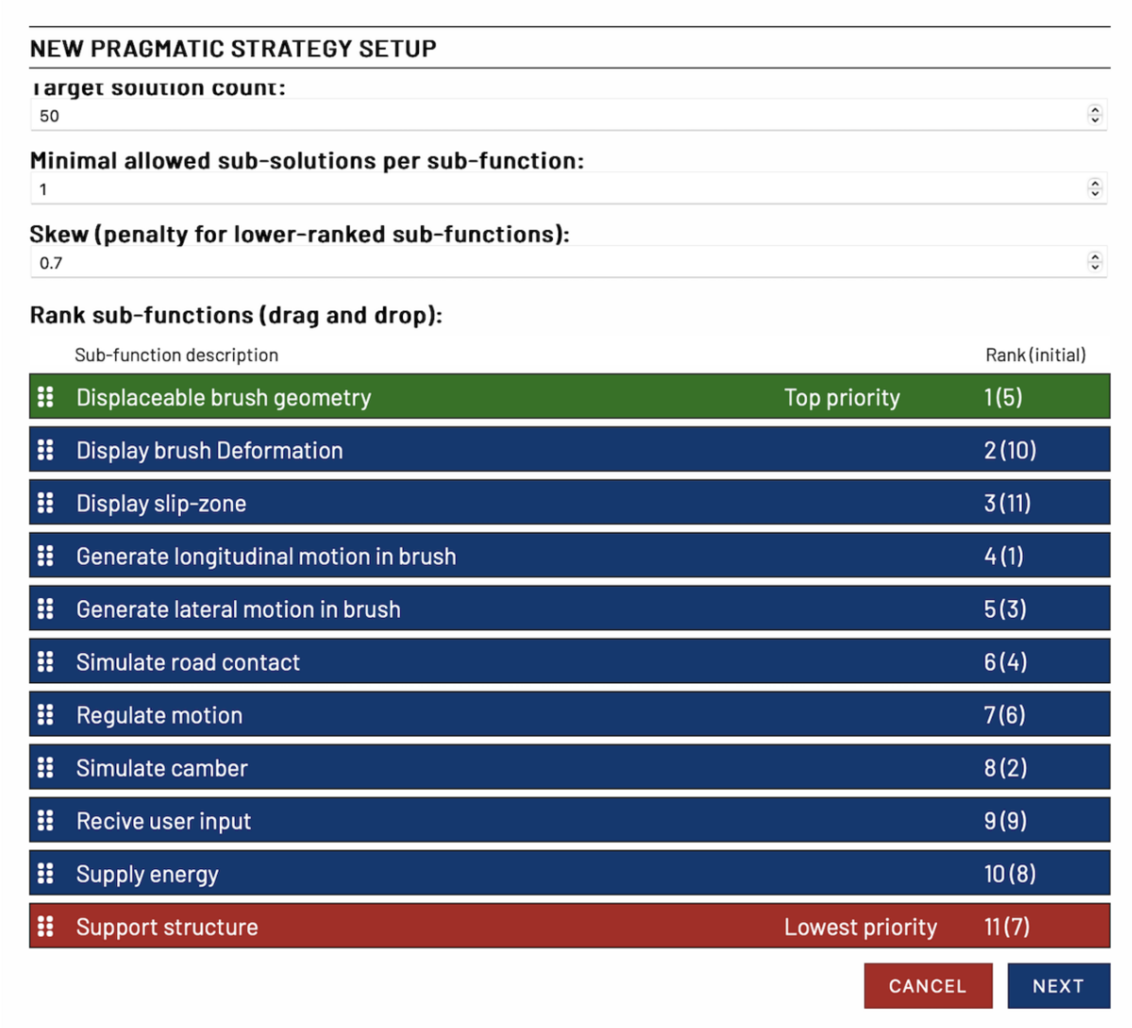

Figure A.2: Pragmatic strategy setup (section 4.2.1)

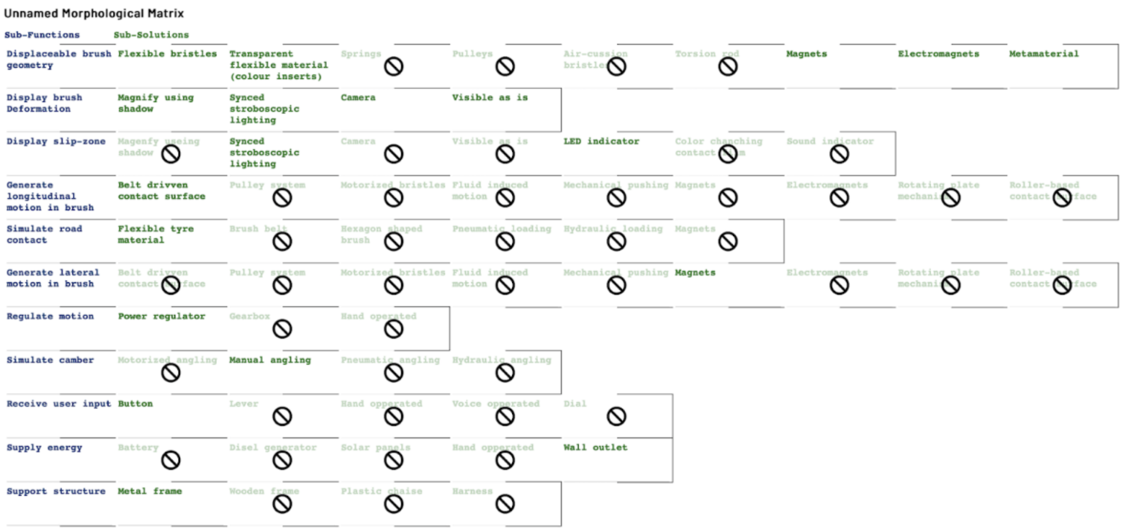

Figure A.3: Initial morphological matrix (section 4.2.1)

Sub-Functions	Sub-Solutions								
Displaceable brush geometry	Flexible bristles	Transparent flexible material (colour inserts)	Springs	Pulleys	Air-cussion bristles	Tortion rod	Magnets	Electro magnets	Meta material
Display brush Deformation	Magenfy useing shadow	Synced stroboscopic lighting	Camera	Visable as is					
Display slip-zone	Magenfy useing shadow	Synced stroboscopic lighting	Camera	Visable as is	LED indicator	Color chanching contact film	Sound indicator		
Generate longitudinal motion in brush	Belt drivven contact surface	Pulley system	Motorized bristles	Fluid induced motion	Mechanical pushing	Magnets	Electromagnets	Rotateing plate mechanism	Rollerbased contact surface
Simulate road contact	Flexible tyre material	Brush belt	Hexagon shaped brush	Pnumatic loading	Hydrolic loading	Magnets			
Generate lateral motion in brush	Belt drivven contact surface	Pulley system	Motorized bristles	Fluid induced motion	Mechanical pushing	Magnets	Electromagnets	Rotateing plate mechanism	Rollerbased contact surface
Regulate motion	Power regulator	Gearbox	Hand operated						
Simulate camber	Motorized angleing	Manual angleing	Phnumatic angling	Hydrolic angleing					
Recive user input	Button	Lever	Hand opperated	Voice opperated	dail				
Supply energy	Battery	Disel generator	Solar panels	Hand opperated	Wall outlet				
Support structure	Metal frame	Wooden frame	Plastic chaise	Harnes					

Figure A.4: Iterated morphological matrix (section 4.2.1)

B

Appendix 2

Functions:

- **Physically visualise brush model (Requirement):** In order for the demonstrator to be an effective teaching tool it needs to be able to clearly demonstrate the bristles and how they interact with the ground in a visual manner.

  Method of verification: Operate the demonstrator and compare the brush behaviour with expected behaviour according to the theory. It doesn't need to be an exact match but it will need to demonstrate steady state conditions and slip conditions.

- **Simulate longitudinal motion (Requirement):** The most basic and fundamental recruitment is demonstrating the bristles deformation during longitudinal motion, it was argued to be the most common motion and thus the most important to demonstrate as well as the easiest one to achieve.

  Method of verification: Operate the demonstrator under pure longitudinal conditions and observe whether the bristles deform in accordance with the expected behaviour.

- **Simulate lateral motion (Desired):** . The ability to simulate lateral motion would allow the demonstrator to show how the bristles deform when the wheel is steered. This would make it possible to visualize how side forces affect the tyre-road contact and how the bristles deform in a direction perpendicular to the rolling direction.

  Method of verification: Tested by "steering the wheel while operating the demonstrator.

- **Simulate camber (Desired):** This would allow the demonstrator to show how wheel inclination affects the contact between the tyre and the road surface. This improves the visualization of tyre behaviour under different wheel angles.

  Method of verification: Operate the demonstrator and compare with theoretical predictions.

- **Collect and compare data with theory (Desired):**A more thorough comparison between the theory and the demonstrator, rather than rough eye measurements and observations. For example, using the theory to calculate exactly when slip conditions occur rather than just showing how the bristles act when they do.

  Method of verification: Calculate and predict different events based on seed and angle of the wheel and compare it to the physical demonstrator.

Performance:

1.1 **Constant slip relation (Desired):** Keeping the speed relation between the bristles and the ground constant would give a more accurate view of the slip phenomena. Too much variation in the speed would impede the ability of the machine to act as a proper demonstrator and educational tool.

Method of verification: Collect speed data to see how stable the relative speed is.

1.2 **Clearly visible deformation from 3 m (required):** To ensure that the demonstrator can be used effectively in an educational setting, it must allow several observers to view the system simultaneously. Therefore, the deformation of the brushes must be clear and easy to observe during operation.

Method of verification: Operate the demonstrator and assess within the group whether the deformation is clearly visible.

1.3 **Clearly visible deformation from 5 m (Desired):** To ensure that the demonstrator can be used effectively in front of a larger group, the brush deformation must remain clearly visible to all observers.

Method of verification: Operate demonstrator and determine among the group if the deformation is visible or not.

1.4 **Clearly visible slip zone 3 m (Desired):** For the same purposes as the deformation, the slip zone would need to be clearly visible.

Method of verification: Operate demonstrator and determine among the group if the slip zone is visible or not.

1.5 **Clearly visible slip zone 5 m (Desired):** For the same purposes as the deformation, the slip zone would need to be clearly visible.

Method of verification: Operate demonstrator and determine among the group if the slip zone is visible or not.

Environment:

2.1 **Environment temperature (Required):** The demonstrator is meant to be used in classrooms and to be stored within Chalmers facilities. Because of this, it needs to be able to handle typical indoor room temperatures without any components breaking or decaying. Therefore, a range of 15 to 30°C was chosen.

Method of verification: Ensure that the recommended operating temperature ranges of all components are verified before integrating into the design.

Size:

The demonstrator should not take up too much space as that might make it difficult to move from place to place as well as complicating storage. But it shouldn't be too small either because it is a visual tool.

3.1 **Maximum length + width + height < 2 m (Required):** This requirement is primarily based on user preferences, as the demonstrator should be easy to handle, transport, and store.

Method of verification: Verify the dimensions using the CAD model as a reference.

3.2 **Maximum length + width + height < 1.5 m (Desired):** This requirement is primarily based on user preferences, as the demonstrator should be easy to handle, transport, and store.

Method of verification: Verify the dimensions using the CAD model as a reference.

Mass:

Like the size, the mass of the object impacts the ability to store and transfer the demonstrator. Because it is only for a quick demonstration it shouldn't be a hassle to move by more than one person or ideally require any special equipment, the lighter the better.

4.1 **Max weight 25 kg (Required):**Based on discussion with supervisors.

Method of verification: weighing the demonstrator

4.2 **Max weight 15 kg (Desired):**Based on discussion with supervisors

Method of verification: Weighing the demonstrator.

Ergonomics:

5.1 **Maximum sound level of 50 dB (Desired):** Based on group discussion

Method of verification: Measure the sound level in decibels while operating the demonstrator under normal working conditions.

Safety

6.1 **Maximum sound level 80 dB (Required):** According to Arbetsmiljöverket [14] the lower exposure action value for daily noise level is 80 dB.

Method of verification: Measure the sound level in decibels while operating the demonstrator under normal working conditions.

6.2 **Minimize projectile debris (Required):** If we look at the demonstrators real life counterpart it can be observed that the wheels of the vehicle might shoot out tiny rocks and other debris during its compression. If a similar event were to occur during the demonstration it might pose a safety hazard as students wanting a closer look might be in the danger zone of being hit by debris at eye level.

Method of verification: Test the demonstrator and see if it emits debris by surrounding it by a light sheet so any notable impact is seen.

6.3 **Minimize risk of fire (Required):** The demonstrator is most likely to run on electricity, which introduces the risk of faulty wiring causing a fire.

Method of verification: Secure cables to prevent them from disconnecting. Inspect the construction and verify that no exposed wires exist and that no wires are at risk for any moving machinery. Be aware of heat generating sources.

6.4 **Minimize risk of electric shock (Required):** The demonstrator is most likely to run on electricity, which introduces the risk of electrical hazards.

Method of verification: Secure cables to prevent them from disconnecting. Inspect the construction and verify that no exposed wires exist and that no wires are at risk for any moving machinery.

6.5 **No sharp edges (Required):** To avoid cutting injuries, there can be no sharp edges.

Method of verification: Inspection of edges.

6.6 **Minimize risk of burns (Required):** Heat may be generated as a result of movement, friction, and electrical components during operation. Therefore, the demonstrator must be designed so that users are not exposed to surfaces with high temperatures.

Method of verification: Verify that no user interaction is required to operate the demonstrator.

6.7 **Minimize pinch hazard (Required):** Reduce risk of pinching or crushing by limiting access to moving parts.

Method of verification: Inspect and test accessibility to moving parts while the demonstrator is unpowered.

Material:

7.1 **Bristles with elastic properties (Required):** The bristles must resemble the properties of the theoretical bristles used in the model. This ensures that the resulting deformation occurs as predicted by the theory.

Method of verification: Existing research, supported by bending and compression tests.

Production cost:

8.1 **Maximum cost 10 000 kr (Desired):** A budget of 10 000 kr has been allocated for the development of the demonstrator.

Method of verification: Cost summery.

Maintenance:

9.1 **Easily replaceable bristles $<$ 60 minutes (Required)** If the design features wear and tear on the bristles, they need to be replaceable. For the demonstrator to be a useful tool, swapping out the bristles can not take too long.

Method of verification: Replace the bristles and measure the time required to complete the process.

9.2 **Easily replaceable bristles $<$ 30 minutes (Desired)** If the design features wear and tear on the bristles, they need to be replaceable. For the demonstrator to be a useful tool, swapping out the bristles can not take too long.

Method of verification: Replace the bristles and measure the time required to complete the process.

Reuse and recycle:

10.1 **Easily repairable:** From both an environmental and economic perspective, the demonstrator should not need to be discarded if an individual component fails.

Method of verification: Permanent joining methods such as gluing, welding, or other irreversible connections should be avoided where possible.

10.2 **Recyclable bristles(Desired):** Because the idea is to be able to replace the bristles it would be ideal if the discarded bristles could be recycled.

Method of verification: Research information regarding the possibilities of recycling the bristles.

C

Appendix 3

Code for motor control

```
const int wheelPin = 9;
const int beltPin = 5;

const int wheelSensor = 3;
const int beltSensor = 2;

// Buttons
const int increaseButton = 8;
const int decreaseButton = 4;

// 6 zones per revolution
const int zonesPerRevolutionWheel = 20;
const int zonesPerRevolutionBelt = 18;

// Gear reduction
const float gearRatio = (20.0 / 74.0) * (20.0 / 74.0);

// Diameters (mm)
const float wheelDiameter = 500.0;
const float beltDiameter = 45.0;

// ========================================
// Correlation target
// ========================================

float targetCorr = 1.0;

// Button states
bool lastIncreaseState = HIGH;
bool lastDecreaseState = HIGH;

// ========================================
// Wheel variables
// ========================================
```

```
int wheelLastState;

bool wheelHasBeenHigh = false;
bool wheelHasBeenLow = false;

float wheelRPM = 0.0;

// ========================================
// Belt variables
// ========================================

int beltLastState;

bool beltHasBeenHigh = false;
bool beltHasBeenLow = false;

float beltRPM = 0.0;

// ========================================
// Wheel PID variables
// ========================================

const float targetWheelRPM = 1.0;

// PID gains
float wheelKp = 80.0;
float wheelKi = 5.0;
float wheelKd = 0.0;

float wheelError = 0.0;
float wheelPreviousError = 0.0;
float wheelIntegral = 0.0;

unsigned long wheelLastPIDTime;

// ========================================
// Belt PID variables
// ========================================

// Slower and more damped PID
float beltKp = 3.0;
float beltKi = 0.3;
float beltKd = 0.5;

float beltError = 0.0;
```

```
float beltPreviousError = 0.0;
float beltIntegral = 0.0;

unsigned long beltLastPIDTime;

// ========================================
// PWM control
// ========================================

int wheelPWM = 77;
int beltPWM = 77;

unsigned long startTime;

unsigned long wheelZoneStartTime;
unsigned long beltZoneStartTime;

void setup()

pinMode(wheelPin, OUTPUT);
pinMode(beltPin, OUTPUT);

pinMode(wheelSensor, INPUT);
pinMode(beltSensor, INPUT);

// Buttons with internal pullups
pinMode(increaseButton, INPUT_PULLUP);
pinMode(decreaseButton, INPUT_PULLUP);

Serial.begin(115200);

wheelLastState = digitalRead(wheelSensor);
beltLastState = digitalRead(beltSensor);

startTime = millis();

wheelZoneStartTime = startTime;
beltZoneStartTime = startTime;

wheelLastPIDTime = startTime;
beltLastPIDTime = startTime;


void loop()

// ========================================
```

```
// Buttons
// ========================================

bool increaseState = digitalRead(increaseButton);

bool decreaseState = digitalRead(decreaseButton);

// Button press = HIGH -> LOW
if (lastIncreaseState == HIGH  increaseState == LOW)

targetCorr += 0.05;

if (targetCorr > 2.0)
targetCorr = 2.0;



if (
lastDecreaseState == HIGH
decreaseState == LOW
)

targetCorr -= 0.05;

if (targetCorr < 0.5)
targetCorr = 0.5;



lastIncreaseState = increaseState;
lastDecreaseState = decreaseState;

analogWrite(wheelPin, wheelPWM);
analogWrite(beltPin, beltPWM);

// ========================================
// WHEEL
// ========================================

int wheelState = digitalRead(wheelSensor);

// HIGH -> LOW
if (
wheelLastState == HIGH
wheelState == LOW
)
```

```
wheelHasBeenHigh = true;


// LOW -> HIGH
if (
wheelLastState == LOW
wheelState == HIGH
)
wheelHasBeenLow = true;


// Calculate wheel RPM
if (
wheelHasBeenHigh
wheelHasBeenLow
)

unsigned long now = millis();

float zoneTime =
(now - wheelZoneStartTime) / 1000.0;

wheelZoneStartTime = now;

float revolutionTime =
zoneTime * zonesPerRevolutionWheel;

float newWheelRPM =
(60.0 / revolutionTime) *
gearRatio;

// Low-pass filter
wheelRPM =
0.8 * wheelRPM +
0.2 * newWheelRPM;

wheelHasBeenHigh = false;
wheelHasBeenLow = false;

// ========================================
// Wheel PID
// ========================================

float dt =
(now - wheelLastPIDTime) / 1000.0;
```

```
wheelLastPIDTime = now;

wheelError =
targetWheelRPM - wheelRPM;

wheelIntegral +=
wheelError * dt;

float derivative =
(wheelError -
wheelPreviousError) / dt;

float output =
wheelKp * wheelError +
wheelKi * wheelIntegral +
wheelKd * derivative;

wheelPWM += output;

wheelPWM =
constrain(wheelPWM, 0, 255);

wheelPreviousError =
wheelError;


wheelLastState = wheelState;

// ========================================
// BELT
// ========================================

int beltState = digitalRead(beltSensor);

// HIGH -> LOW
if (
beltLastState == HIGH
beltState == LOW
)
beltHasBeenHigh = true;


// LOW -> HIGH
if (
beltLastState == LOW
beltState == HIGH
```

```
)
beltHasBeenLow = true;


// Calculate belt RPM
if (
beltHasBeenHigh
beltHasBeenLow
)

unsigned long now = millis();

float zoneTime =
(now - beltZoneStartTime) / 1000.0;

beltZoneStartTime = now;

float revolutionTime =
zoneTime * zonesPerRevolutionBelt;

float newBeltRPM =
60.0 / revolutionTime;

// Low-pass filter
beltRPM =
0.8 * beltRPM +
0.2 * newBeltRPM;

beltHasBeenHigh = false;
beltHasBeenLow = false;

// ========================================
// Belt PID
// ========================================

float targetBeltRPM =
wheelRPM *
(wheelDiameter / beltDiameter) *
targetCorr;

float dt =
(now - beltLastPIDTime) / 1000.0;

beltLastPIDTime = now;

beltError =
```

```
targetBeltRPM - beltRPM;

beltIntegral +=
beltError * dt;

// Anti-windup
beltIntegral =
constrain(
beltIntegral,
-50,
50
);

float derivative =
(beltError -
beltPreviousError) / dt;

float output =
beltKp * beltError +
beltKi * beltIntegral +
beltKd * derivative;

beltPWM += output;

// Prevent motor stall
beltPWM =
constrain(beltPWM, 40, 255);

beltPreviousError =
beltError;

// ========================================
// Print
// ========================================

float wheelTangential =
wheelRPM * wheelDiameter;

float beltTangential =
beltRPM * beltDiameter;

float tangentialCorrelation =
beltTangential / wheelTangential;

Serial.print("Wheel RPM: ");
Serial.print(wheelRPM);
```

```
Serial.print(" | Belt RPM: ");
Serial.print(beltRPM);

Serial.print(" | Corr: ");
Serial.print(tangentialCorrelation);

Serial.print(" | Target Corr: ");
Serial.print(targetCorr);

Serial.print(" | Wheel PWM: ");
Serial.print(wheelPWM);

Serial.print(" | Belt PWM: ");
Serial.println(beltPWM);


beltLastState = beltState;

delay(2);
```

DEPARTMENT OF MECHANICS AND MARITIME SCIENCES
CHALMERS UNIVERSITY OF TECHNOLOGY
Gothenburg, Sweden
www.chalmers.se

CHALMERS